AD-A044 737 STANFORD RESEARCH INST MENLO PARK CALIF F/G 20/14

OBSERVED CHARACTERISTICS OF IONOSPHERICALLY PROPAGATED HF ATMOS--ETC(U)

MAY 77 W B ZAVOLI

UNCLASSIFIED NL

1 OF 2

ADA044737

2

B.S.

9

Technical Report

6

OBSERVED CHARACTERISTICS OF IONOSPHERICALLY PROPAGATED HF ATMOSPHERICS FROM NORMAL AND SEVERE THUNDERSTORMS

10

By: WALTER B. ZAVOLI

11 May 77

Prepared for:

STANFORD RESEARCH INSTITUTE

12 49 p.

Under:

INDEPENDENT RESEARCH AND DEVELOPMENT (IR&D)
PROJECT 658D32-CIK

Distribution of this report is unlimited. It may be cited in the literature.

STANFORD RESEARCH INSTITUTE
Menlo Park, California 94025 · U.S.A.

332 500 LB

STANFORD RESEARCH INSTITUTE
MENLO PARK, CALIFORNIA 94025
(415) 326-6200

16 September 1977

To: Distribution

Subject: New information on the characteristics of HF atmospherics radiated by lightning flashes, when received at over-the-horizon distances on a highly directional antenna of the type used for HFDF and for OTH radar systems.

Because you routinely receive our reports on over-the-horizon (OTH) radar prepared under Contract N00014-75-C-0930, we believe that the enclosed technical report prepared under an SRI International independent research and development (IR&D) project will be of interest to you.

The thrust of this work is to understand better the characteristics of HF electromagnetic noise radiated by thunderstorms, as received at over-the-horizon distances by a highly directional antenna. The findings should be of direct interest in HFDF and OTH radar applications whenever background noise levels determine system performance.

In particular, these findings can affect the design of nonlinear circuits used to reduce the effects of noise spikes, and the design of adaptive antennas used to limit the effects of spatially fixed noise and other interference. Here nonlinear circuits include clippers, limiters, and noise-excision techniques made practical by digital computers.

The report, "Observed Characteristics of Ionospherically Propagated HF Atmospherics from Normal and Severe Thunderstorms," was prepared by Dr. Walter B. Zavoli, who used the Wide Aperture Research Facility (WARF) operated by SRI in support of OTH radar studies sponsored by the Office of Naval Research and by the Electronic Systems Division, Air Force Systems Command.

Some important conclusions of this work can be summarized as follows:

- A highly directional antenna can be thought of as a different way to view the thunderstorm environment; it has the effect of bringing distant flashes close up. Waveshape is preserved in this process--at least over bandwidths of practical interest--so the noise output of a receiver connected to a directional antenna will be far more impulsive in nature, and less Gaussian, than the output of a receiver connected to a less-directional antenna.

- A new class of atmospheric has been identified. This class seems to be associated with the transition of a normal thunderstorm into a severe one (i.e., one which produces hail, funnel

clouds, and/or tornadoes). At close (line-of-sight) ranges these atmospherics tend to be masked by other aspects of the electromagnetic radiation from storms, and thus seem to have been missed in prior studies. But at OTH distances, assuming sufficient antenna directivity, the atmospherics are distinctive. Thus they offer the promise of a new means for identifying, studying, and possibly tracking, storms whose intensity can reach a point which makes them a threat to lives, property, or the success of military operations.

- A further unanticipated finding is that single lightning flashes from normal thunderstorms cannot be considered to be an electrical point source for highly directive HF antennas. For example, radiation (actually, a succession of discharges) from a typical lightning flash occurring over 1000 km from the WARF antenna was shown to change its bearing by roughly one degree during the duration of the flash. These bearing fluctuations are presumably the result of the successive discharging of various charged volumes within a cloud or system of clouds; such behavior could have a significant effect on the performance of adaptive antennas and on the design of algorithms chosen to reduce or eliminate the effects of spatially fixed noise.

Dr. Zavoli will of course welcome any comments or discussion of his work. He may be contacted by mail at SRI International, Building 320A, 333 Ravenswood Avenue, Menlo Park, California 94025, or by telephone at (415) 326-6200, extension 2393.

Sincerely yours,

L. E. Sweeney, Jr.
Director
Remote Measurements Laboratory

LES:jk

Encl. "Observed Characteristics of Ionospherically Propagated HF Atmospherics from Normal and Severe Thunderstorms," by Walter B. Zavoli, Technical Report, SRI International IR&D Project 658D32-CIK, May 1977.

Distribution List

DEPARTMENT OF DEFENSE

Organization	No. of Copies
Director Defense Advanced Research Projects Agency ATTN: STO, Mr. Eugene H. Kopf 1400 Wilson Boulevard Arlington, Virginia 22209	1
Office of the Deputy Assistant Secretary (Intelligence and Warning Systems) Pentagon, Room 3E282 Washington, D.C. 20301	1
Office of the Deputy Director Research and Advanced Technology DDR&E Pentagon, Room 3E114 Washington, D.C. 20301	1
Office of the Assistant Director Defensive Systems, DDR&E ATTN: LTC Edward D. Cohen, USAF Pentagon, Room 3D136 Washington, D.C. 20301	1
Director Defense Intelligence Agency ATTN: DC7 DT23 Pentagon Washington, D.C. 20301	 1 1
Director National Security Agency ATTN: R5, Mr. J. G. Hengen/ Dr. John Pinkston W23, Major R. M. McCormick W32, Mr. C. H. Wilts/ Dr. Lee Edwards Fort Geo. G. Meade, Maryland 20755	 1 1 1
Commandant Defense Intelligence School Washington, D.C. 20374	1
Defense Documentation Center Cameron Station Alexandria, Virginia 22314	2
Director Weapons Systems Evaluation Group 400 Army-Navy Drive Arlington, Virginia 22202	1

DEPARTMENT OF THE NAVY

Organization	No. of Copies
Office of Naval Research ATTN: Code 427, Dr. Henry Mullaney Code 461(FP), Mr. J. J. Kane 800 N. Quincy Street Arlington, Virginia 22217	 1 1
Office of Naval Research Branch Office ATTN: Mr. Stan Curley 495 Summer Street Boston, Massachusetts 02210	1
Office of the Assistant Secretary of the Navy (R&D) ATTN: Dr. Thomas P. Quinn Pentagon, Room 4E741 Washington, D.C. 20350	1
Office of the Chief of Naval Operations ATTN: OP-955D/ Capt. B. F. Czaja, USN Pentagon, Room 5D625 Washington, D.C. 20350	1
Office of the Chief of Naval Operations ATTN: OP-942/ Capt. F. R. Fahland, USN OP-098TE Pentagon Washington, D.C. 20350	 1 1
Commander-in-Chief, U.S. Atlantic Fleet Norfolk, Virginia 23511	1
Commander-in-Chief U.S. Pacific Fleet ATTN: Code 302 Makalapa FPO San Francisco, California 96610	1
Commander, Third Fleet ATTN: Code N22 Code N7644, Mr. F. Forsyth Code OIT Ford Island FPO San Francisco, California 96610	 1 1 1

Organization	No. of Copies
Chief of Naval Material	
ATTN: NMAT 0311,	
Cdr. J. W. Hugo, USN	1
2211 Jefferson Davis Highway	
Arlington, Virginia 20360	
Commander	
Naval Ocean Systems Center	
ATTN: Code 0104, Dr. Paul Moose	1
Code 1201, Mr. W. L. Hastings	1
Code 7141, Mr. H. J. Wirth	1
Code 721, Dr. Peder M. Hanson	1
Code 722, Mr. V. E. Hildebrand	1
San Diego, California 92152	
Commander	
Naval Electronic Systems Command	
ATTN: 03/03A	1
034/034A	1
320A/Mr. M. Lewis	1
3201	1
52011A/Mr. G. N. Skillicorn	1
52023B/Mr. R. D. Blackburn	1
National Center No. 1	
2511 Jefferson Davis Highway	
Arlington, Virginia 20360	
Commander	
Naval Missile Center	
ATTN: Code N03022	1
Point Mugu, California 93041	
Commander	
Naval Ocean Research and Development Activity	
ATTN: Code 600, Dr. R. D. Gaul,	
Director, LRAPP	1
Bay St. Louis, Mississippi 39529	
Director	
Naval Research Laboratory	
ATTN: Technical Information Div.	1
Code 5300	1
Code 5320/Mr. J. M. Headrick	1
Code 5400/5432C	1
Code 5464/Dr. J. R. Davis	1
Washington, D.C. 20390	
Commander	
Naval Security Group Headquarters	
ATTN: SCOE (NRAC)	1
3801 Nebraska Avenue, N.W.	
Washington, D.C. 20390	
Commander	
Naval Weapons Center	
ATTN: Code 3524, Mr. R. S. Hughes	1
Code 127, Mr. D. Witcher	1
China Lake, California 93555	

Organization	No. of Copies
Officer-in-Charge	1
Navy Field Operational Intelligence Office	
Fort Geo. G. Meade, Maryland 20755	
Director	1
Navy Ocean Surveillance Information Center	
Suitland, Maryland 20390	
Commandant of the Marine Corps	
ATTN: Code RD-1,	
Dr. A. L. Slafkosky	1
Washington, D.C. 20380	
Center for Naval Analyses	
ATTN: Dr. Gary Phillips	1
1401 Wilson Boulevard	
Arlington, Virginia 22209	
DEPARTMENT OF THE AIR FORCE	
Office of the Assistant Secretary of the Air Force (R&D)	
ATTN: SAF/RD, Dr. Albert C. Vosburg	1
Pentagon, Room 4D977	
Washington, D.C. 20330	
Headquarters, USAF	
ATTN: AFRDPE,	
Maj. F. J. Caravaglio, USAF	1
AFINY	1
Pentagon	
Washington, D.C. 20330	
Headquarters	
Research and Technology Division	
Air Force Systems Command	
ATTN: DLC	1
SDED	1
Andrews AFB, Washington, D.C. 20331	
Headquarters	
Electronic Systems Division	
Air Force Systems Command	
ATTN: OCS, 414L SPO	3
OCSE	1
OCSX	1
Hanscom AFB, Massachusetts 01731	
Headquarters	
Air Force Geophysics Laboratory (AFSC)	
ATTN: LIB	1
Hanscom AFB, Massachusetts 01731	

Organization	No. of Copies
Headquarters Rome Air Development Center ATTN: OCSE OCSL Griffiss AFB, New York 13442	 1 1
Headquarters Rome Air Development Center ATTN: ETEI Hanscom AFB, Massachusetts 01731	 1
Headquarters Foreign Technology Division Air Force Systems Command ATTN: ENDP ENDA PDJL Wright Patterson AFB, Ohio 45433	 1 1 1
Headquarters Aerospace Defense Command ATTN: XPAS Ent AFB, Colorado 80912	 4
Headquarters, SAC ATTN: DOKS XPF Offutt AFB Omaha, Nebraska 68113	 1 1
Headquarters 4754 RADES/DVS ATTN: Dr. George Parker Hill AFB, Utah 84401	 1
Headquarters Air Weather Service ATTN: AWS/DNP Scott AFB, Illinois 62265	 1
Headquarters USAF Security Service ATTN: USAFSS/XRS San Antonio, Texas 78241	 1
DEPARTMENT OF THE ARMY	
Director Ballistic Missile Defense Advanced Technology Center ATTN: BMDATC-D, Mr. Frank L. Brown Huntsville, Alabama 35807	 1
Commander U.S. Army INSCOM Arlington Hall Station ATTN: IARDA-OS Arlington, Virginia 22212	 1

Organization	No. of Copies
Commander U.S. Army Garrison Vint Hill Farms Station ATTN: IAVOP-AF Warrenton, Virginia 22186	 1
OTHER	
Barry Research ATTN: Dr. R. B. Fenwick 767 North Mary Sunnyvale, California 94085	 1
Environmental Research Institute of Michigan P. O. Box 618 Ann Arbor, Michigan 48107	 1
General Electric Company Heavy Military Electronics System ATTN: Mr. Gary R. Nelson P. O. Box 1122, Court Street Plant 4-1 Syracuse, New York 13201	 1
GTE Sylvania, Inc. Electronic Systems Group - ED ATTN: Mr. J. Page 77 A Street Needham, Massachusetts 02194	 1
GTE Sylvania, Inc. Electronic Systems Group - WD ATTN: Mr. Larry Fowler P. O. Box 205 Mountain View, California 94040	 1
Massachusetts Institute of Technology Lincoln Laboratory ATTN: Dr. R. M. O'Donnell, Group 43 P. O. Box 73 Lexington, Massachusetts 02173	 1
MITRE Corporation ATTN: Mr. William Talley Mr. Samuel Hunt Mr. D. J. Marino Route 62 and Middlesex Turnpike Bedford, Massachusetts 01730	 1 1 1
NOAA Laboratories ATTN: ERL R45x5/ Dr. Donald Barrick Boulder, Colorado 80302	 1

Organization	No. of Copies	Organization	No. of Copies
Radio Corporation of America ATTN: Dr. R. W. Roop Borton Landing Road Moorestown, New Jersey 08057	1		
RAND Corporation ATTN: Dr. Cullen Crain 1700 Main Street Santa Monica, California 90406	1		
Raytheon Company Boston Post Road ATTN: Mr. L. C. Edwards Wayland, Massachusetts 01778	1		
Raytheon Company Sudbury Engineering Facility ATTN: Mr. D. Odom 528 Boston Post Road Sudbury, Massachusetts 01776	1		
Riverside Research Institute ATTN: Mr. R. Mastrandrea 80 West End Avenue New York, New York 10023	1		
Sanders Associates ATTN: Mr. Sidney M. Bennett Mr. Robert A. Palmer 95 Canal Street Nashua, New Hampshire 03060	1 1		
Stanford Research Institute ATTN: Mr. John Schlobohm/ Dr. John Ames 333 Ravenswood Avenue Menlo Park, California 94025	1		
U. S. Department of Commerce Office of Telecommunications ATTN: Dr. William Utlaut Mr. L. H. Tventen, 4401.210 Institute for Telecommunication Science Boulder, Colorado 80302	1 1		
University of Colorado Office of Contracts and Grants ATTN: Ms. Virginia Stone for Prof. Lloyd J. Griffiths Administrative Annex, Willard 380 Boulder, Colorado 80302	1		

ABSTRACT

Using a directional HF antenna with a nominal beamwidth of 0.5 deg, atmospherics from midwestern thunderstorms classified as severe, and thus likely to produce tornadoes, were studied in California. The antenna was scanned across regions within a one-hop propagation distance likely to develop tornadoes at the time of the test. These regions were selected on the basis of National Weather Service severe weather forecasts. The existence of strong propagation from these regions at the radio frequencies used was verified by means of backscatter soundings.

Analysis of the data recorded in those directions and periods for which severe storm events were reported led to the discovery of a class of radio atmospherics significantly different from those radiated during normal thunderstorm activity. Atmospherics of this new type take the form of randomly occurring impulses having certain distinctive characteristics. A technique was devised to extract this class of atmospherics from the remaining radio noise background. Based on 23 hours of data, taken on four separate days, a statistically significant correlation between the reception of these impulses and the presence of remote severe thunderstorms was found.

Comparison with HF line-of-sight measurements performed by others shows that, as a class, these atmospherics were very unlikely to have been previously recognized as a significant subclass within the total atmospheric activity present during severe storms. Subsequent analysis found that the temporal distribution of these atmospherics can be closely approximated by a Poisson model having a slowly varying mean. It is the increase in this mean rate which correlates with observed severe storm events such as tornadoes, funnel clouds, and severe hail. Finally, a hypothesis is presented suggesting concentrated wind shears within the storm as the most probable mechanism for generating the observed atmospherics.

This research was initially motivated by the observation of strong and detailed atmospheric waveforms received on the directional antenna, despite the absence of local thunderstorm activity. Comparison of atmospheric noise simultaneously received with this antenna and with an omnidirectional antenna suggested that these atmospherics were from normal thunderstorms of remote origin, lying within the directional antenna's main beam. Direct verification was obtained when measurements taken close to a New Mexico thunderstorm correlated with simultaneous measurements taken 1300 km away with the directional antenna.

The directional antenna was then reconfigured so as to receive in eight contiguous directions simultaneously. This revealed readily measureable changes in the angle of arrival of atmospheric noise radiated from the many small discharges associated with a single lightning flash. It would therefore appear that variations in horizontal location of in-cloud charge centers involved in individual remote lightning flashes can be measured in this way. The average horizontal extent of individual flashes measured from one storm was 9 ± 4 km.

CONTENTS

ILLUSTRATIONS

TABLES

ACKNOWLEDGMENTS

I would like to express thanks to Professor O. G. Villard, Jr. for his ample support and guidance throughout this research project. I wish also to extend thanks to Professors A. M. Peterson and M. Flynn for their suggestions in improving the quality of this dissertation. I am indebted to Drs. E. T. Pierce and N. Cianos for their insights in atmospheric electricity. Lastly, I am grateful to Mr. C. Powell and Mr. W. Preuss for their efforts in collecting data as well as to Ms. J. King for her help in preparing this manuscript.

This work was accomplished with the use of facilities made available to SRI by the Office of Naval Research and the Air Force Systems Command. Technical assistance was provided by the Naval Weather Service Environmental Detachment, U.S. Naval Air Station, Moffett Field, California; the San Francisco branch of the National Weather Service; and the National Severe Storms Forecast Center, Kansas City, Missouri.

I INTRODUCTION

A. Purpose

The purpose of this research was to investigate experimentally characteristics of high frequency, HF, atmospherics of remote origin. A directional antenna was used to study atmospherics from severe thunderstorms occurring several thousand kilometers from the receiving apparatus. The term "atmospheric" is used here as defined by Horner--that is, the electromagnetic energy radiated from any electrical breakdown occurring during a single lightning flash.[1*] A single atmospheric can be a simple impulse, an impulse train, or a continuous waveform. Atmospheric noise is the superposition of atmospherics from many lightning flashes.

B. Motivation

Individual atmospherics, strong compared to the background noise and apparently originating at skywave distances,[†] have often been received on a directional antenna situated in northern California. This antenna, part of the Wide Aperture Research Facility (WARF)[3,4] was designed by Sweeney[5] and successfully used by Barnum,[6] Washburn[7] and others to investigate properties of the ionosphere and HF radio propagation. For such research, strong atmospherics were a source of annoyance, and techniques such as those described by McKinney and Zavoli[8] have been devised to mitigate their effects. Considering the absence of close-by thunderstorm activity, the strength and detailed structure of these atmospherics (which were not observed on an omnidirectional antenna) suggested to the author that the directional properties of the WARF antenna might be used to investigate remote atmospheric electricity.

---

*References are listed at the end of this dissertation.

†For the HF band, skywave propagation (reflection from the ionosphere) can occur for distances substantially beyond the horizon. Propagation paths using a single ionospheric reflection (i.e., a one-hop path) can occur over distances of 200 to 4000 km. Fundamentals of ionospheric radio propagation can be found in Davies.[2]

In the past, atmospherics have been used to study the physical mechanisms of the lightning discharge. These studies have concentrated on line-of-sight lightning to maximize sensitivity, eliminate propagation effects, and correlate electrical measurements with optical records. For the most part, the component of atmospherics below 100 kHz has been used because of its strength and the relatively small number of impulses radiated per flash.

Prior to the current work, little research had been conducted using remote (i.e., skywave-propagated) HF atmospherics. Horner[9] pointed out the difficulties associated with obtaining meaningful records of individual HF atmospherics of remote origin. In general, such signals are weaker than their VLF counterparts. Since HF atmospherics contain many more impulses (several hundred), the chances are greater for overlap (the simultaneous reception of atmospherics from different flashes). However, as demonstrated by the results described in this dissertation an antenna such as that at WARF has sufficient directivity and sidelobe rejection to overcome these difficulties by increasing signal-to-noise ratio (SNR) and reducing event overlap on in-beam atmospherics. These capabilities enable the WARF antenna to gather useful information from remote lightning and thus study normal and severe thunderstorm activity. Furthermore, the flexibility to point the antenna in any direction of current interest and take measurements from a distance avoids the difficult problem of trying to be at the right place at the right time (i.e., under an active thunderstorm of interest). This capability is particularly useful in the study of the more elusive severe thunderstorms where research is slowed by these logistics difficulties. The thrust of the research described here was first a general investigation of the properties of atmospheric noise received on the directional WARF antenna, and then a study of remote normal and severe thunderstorm activity through reception of atmospherics.

C. Background

By the start of this century, the state of knowledge of atmospherics paralleled knowledge of the physics of lightning; each contributing to the understanding of the other. Physics, meteorology, powerline engineering, and radio science were the principal disciplines involved in the study of lightning and its electromagnetic radiation.

A brief history of early lightning research is presented below. The study of atmospherics is then surveyed, with emphasis placed on HF research pertinent to the current work. Finally, the previous research on atmospherics associated with severe thunderstorms is reviewed. Comprehensive descriptions of thunderstorms and the lightning process may be found in works written by Viemeister,[10] Malan,[11] and Uman.[12]

1. Early Lightning Research

Sir Isaac Newton and another English scientist, William Wall, were among the first to write of the resemblance between electricity and lightning. But the electrical nature of thunderstorms was not verified until Benjamin Franklin's celebrated kite experiment of June 1752.* Besides the practical invention of the lightning rod, few major advances in the understanding of lightning were made over the next century. In 1879 Thomas A. Edison invented the light bulb, and by 1882 the first electric power lines had been built. These were often struck (or narrowly missed) by cloud-to-ground lightning flashes. The resulting current surges propagated along the power lines and damaged equipment. Power-line engineers sought to measure the peak and duration of these current surges in order to devise methods of neutralizing their destructive effects. Unfortunately, equipment for studying such transient phenomena were not then available.

---

*D'Alibard succeeded in proving the electrical nature of lightning two months earlier in France. Since the experiment he performed had been designed and published by Franklin, the discovery has been attributed to the latter.

In 1922 Norinder adopted DuFour's invention of the cathode-ray oscillograph to photograph lightning-induced electrical transients. During the next decade this device was used to obtain an understanding of the transient nature of lightning. With this knowledge the lightning arrester was perfected for power-line protection.

The next series of contributions can be traced back to the research of Schonland and his associates in South Africa. In 1933 they modified Boys' invention of the rotating camera to successfully obtain optical records of lightning with extremely fast time resolution. Over the next 15 years, analysis of their photographic records coupled with simultaneous electromagnetic measurements formed the basis of our current understanding of the cloud-to-ground lightning discharge.

2. Previous Work on the Study of Atmospherics

Even before the invention of the wireless, Marconi was aware of radio noise caused by lightning; for the Russian meteorologist Popov had used an invention remarkably similar to Marconi's to receive atmospherics for studying thunderstorms. The earliest research using atmospherics to understand thunderstorm electrification was performed by Watson-Watt[13] and Appleton.[14] Their studies were conducted at ELF where atmospherics are principally associated with the return strokes in a cloud-to-ground discharge. These atmospherics can be characterized as very strong pulses lasting about 150 μs.

Schonland[15] recognized that optical measurements were insufficient to characterize totally the electrical phenomena of lightning. Accordingly, he took simultaneous photographic and electrical measurements of close lightning. His associate, Malan,[16] was the first to attempt to correlate the structure of close atmospherics at different frequencies. He found that at frequencies above VLF the structure of the atmospheric waveform changed. The return stroke was no longer the dominant source of radiation. In fact, at HF a 10-to-15-ms quiet period followed each return stroke. During the res of the flash, HF noise radiated nearly continuously, and intra-cloud discharges radiated as much noise as cloud-to-ground flashes.

Horner[17,18] made a more comprehensive study of close-by atmospherics at different frequencies. In particular he showed that, in disagreement with current theory, HF atmospheric waveforms could not be accounted for strictly by return strokes and stepped leader processes. He suggested that the in-cloud processes occurring during the intervals between return strokes were the cause of most HF radiation.

Using receiver bandwidths of over 100 kHz, Oetzel and Pierce[19] found that HF atmospherics were comprised of several hundred to over a thousand impulses. The bandwidth of typical HF communications receivers is too narrow to resolve this impulse train. Thus at the output of such a receiver an HF atmospheric usually takes the form of a nearly continuous burst of noise.

During the 1950s, research was conducted to develop statistical descriptions of atmospheric noise for designing modern communications equipment and modulation formats. Since atmospherics often produce the dominant noise source below 20 MHz, HF noise was included in this study. The fact that individual HF atmospherics often overlapped and thus could not be distinguished was of no concern here, since the object was to characterize the noise background. Crichlow et al.[20] developed an empirical model of the amplitude probability distribution of atmospheric noise received on an omnidirectional antenna. Others have used the slightly less accurate but more tractable lognormal distribution to characterize atmospheric noise. Various statistical models of the lightning radiation process were developed for describing the temporal character of atmospheric noise. Of these, the impulsive noise model of Hall's[21] has been considered accurate, particularly for VLF. The Poisson-Poisson model of Furutsu and Ishida[22] is also appropriate for modeling atmospheric noise at HF.

Schonland[15] realized the potential benefits of receiving remote atmospherics. From a single station, information could be gathered from many storms at various distant locations. However, until the present work, remote measurement programs have concentrated on VLF atmospherics. Because of their strength and their ability to

propagate over long distances without great attenuation, they can be easily received. And because they take the form of a few impulses per flash, chances remain high that individual impulses of atmospherics from different storms will not overlap. The principal source of information derived from these measurements has been the location of remote thunderstorms. Using a network of VLF direction finders, the British have been successful in monitoring the location of thunderstorms over portions of northern Europe and the North Atlantic.

Horner[1] pointed out that the structure of HF atmospheric noise would become more variable when received on a directional antenna. Ortenberger[23] used this principle to show that the level of atmospheric noise received on a directional antenna could vary substantially with direction. To the author's knowledge, Horner[9] made the only previous attempt to infer specific information from individual HF atmospherics propagated via skywave. Receiving the same atmospheric at different HF frequencies he was able to use predictions of propagation conditions to estimate the range to the flash to an accuracy of 100 km.

3. Atmospherics Associated with Severe Thunderstorms

With the appropriate meteorological conditions, thunderstorms can develop giant proportions. These thunderstorms are classified as severe if they produce at least one of the following: a tornado, funnel cloud, waterspout, hail (greater than 0.75 inch diameter), wind gusts (greater than 50 knots), or extreme upper air turbulence. The intensely active electrical nature of severe storms has often been noted and unusual lightning has even been observed within the actual tornado vortex.[24] In 1950, Jones[25] reported that VLF atmospherics radiated from severe thunderstorms exhibit identifiable characteristics, thus suggesting a potential mechanism for severe thunderstorm warnings.

Under Project Tornado-Spherics[26] the Air Force studied 10-kHz atmospherics and observed unusually high numbers of atmospherics about one hour prior to tornado sightings. Typically, the rate of atmospherics returned to normal prior to tornado formation. Jones[27] found that atmospheric rates at 150 kHz were a more sensitive indicator of tornado

activity. Rates at this frequency were unusually high before and during known tornadoes. He also observed a localized region of intense lightning activity within the parent cloud and suggested that this "pulse generator" was the origin of this unusual electrical activity. On the other hand, Scouten[28] found atmospherics received on a 150-kHz direction finder to be distributed over a wider region within the parent cloud centered about the vortex.

Silberg[29] studied the radiation spectrum of atmospherics from severe thunderstorms and found it did not decrease with frequency as fast as for atmospherics from normal thunderstorms. In 1968 Weller published a news article suggesting that home TV sets could be used to warn of close tornadoes. Biggs and Waite[30] studied the cause of TV-tornado detections and found a significant VHF component in atmospherics from close tornadoes. Stanford[31] and Lind[32] further investigated severe thunderstorm atmospherics over a range of frequencies. They found frequencies above 1 MHz to be most responsive to severe storm activity.

In the early 1970s Taylor[33] correlated tornado activity with the rate of bursts of atmospheric impulses for radio frequencies ranging from VLF to HF. In order to compare observations of these different frequencies he had to account for the fact that the number of impulses radiated by a lightning flash increased with increasing frequency. At VLF a normal cloud-to-ground discharge will produce about ten impulses, while the same flash may radiate as many as 10^4 impulses at HF. Using fast logic circuitry, Taylor counted the rate of impulses at different amplitude thresholds for frequencies between 10 kHz and 3 MHz. When an impulse rate momentarily exceeded the receiving frequency measured in kilohertz a "burst" was counted. Taylor found that at frequencies greater than 1 MHz a burst rate about 20 per minute suggested the presence of a severe thunderstorm.

Based on these results, Taylor[34] constructed several atmospherics receivers to record the 3-MHz burst rates of storms. These units were deployed throughout the Great Plains during the 1972 and 1973 tornado seasons. While the correlation between tornadoes and high burst rates was strong, there was also a disturbingly high

false-alarm rate. This was partially attributed to the counting of atmospherics from all storms within the reception area. In an effort to reduce this problem, some directional discrimination was provided. With this new equipment, burst rates for eight 45^{o} azimuth sectors could be calculated independently. Preliminary analysis of data recorded using this technique shows a substantial reduction in false alarms with no change in detection rates.

D. Approach Used in the Present Study

The use of HF atmospherics to study remote meteorological processes has previously been neglected. Propagation uncertainties and confusion arising from the reception of overlapping events combined to discourage their use. In the research described here, a directional HF antenna and on-line ionospheric soundings were used to diminish these difficulties.

The initial phase of this research was directed toward verifying that convolution of the WARF antenna pattern with a typical summertime atmospheric noise environment would result in the strong reception of remote atmospherics. A field experiment was conducted to obtain experimental verification that atmospherics received on the WARF antenna were from lightning at a one-hop distance. To the author's knowledge, results from this test represent the first time the sources of remote HF atmospherics were positively located through simultaneous electrostatic field measurements taken within line of sight of the lightning.

Subsequent emphasis was placed on the study of HF atmospherics from remote severe thunderstorms. Data gathered during this phase of the research revealed a previously undiscovered class of HF atmospherics associated with severe thunderstorms. A technique was developed to extract this component from other types of atmospheric waveforms. The results were statistically analyzed, confirming the correlation between the reception of these atmospherics and the presence of severe thunderstorm events. These atmospherics were next compared with line-of-sight measurements of HF atmospherics associated with severe storms. Finally, their temporal characteristics were studied and the results were used to postulate what meteorological factors might be their cause.

E. Original Contributions

The research described here makes original contributions to the study of remote severe thunderstorm activity and to the understanding of HF atmospherics received on directional antennas. Specifically:

(1) A new class of HF atmospherics was discovered that were statistically correlated with the occurrence of remote severe thunderstorms. This class of atmospherics has not previously been isolated by line-of-sight measurements although their short duration (lasting for less than the receiver response time of 0.7 ms) make them easily distinguishable from bursts of HF impulses associated with atmospherics from lightning in normal storms. Based on a 12-dB SNR threshold, the rate of these severe storm atmospherics was most commonly observed at 120 per minute during periods of severe storm activity. In contrast, a rate of 20 per minute was commonly observed for periods without severe activity. The temporal distribution of these atmospherics was found to approximate that of a Poisson process.

(2) It was shown that individual HF atmospherics from remote lightning can be received on a directional antenna with sufficient strength and detail to be used to study these remote lightning flashes. For example, the type of flash (e.g., cloud-to-ground or intra-cloud) and the rate of occurrence of return strokes were measured from the temporal properties of these atmospherics.

Also, variations in the direction of arrival of individual atmospherics were used to infer the horizontal dimension of the region within a storm cloud that is electrically active during a flash. For a storm occurring over New Mexico, the average horizontal dimension of the electrically active region was found to be 9 ± 4 km.

II ANTENNA FACILITIES AND EQUIPMENT USED IN THE PRESENT RESEARCH

A. Directional Antenna

The principal tool used throughout this research was a directional HF antenna--part of the Wide Aperture Research Facility (WARF). This antenna, shown in Figure 1, is a 2.5-km linear broadside array consisting of 256 vertical monopoles. As seen from Figure 2, the array, situated in northern California, can be steered $\pm 32^{\circ}$, in 0.25° steps, from its boresite direction of true east (or west, since it is fully bidirectional).* Steering is achieved by electronically adding varying lengths of cable into elemental paths of the analog beamforming apparatus. The antenna's beamwidth and directivity vary with frequency and steer angle. A nominal 3-dB beamwidth of 0.5° is achieved for a boresite steer and a midband frequency of 15 MHz. A plot of the theoretical antenna pattern for the above values is reproduced in Figure 3.

This antenna as well as a close-by single vertical monopole were used for recording HF noise. The data were received on equipment built at SRI for general use in WARF experiments. Data for the experiments described here were recorded on analog and digital magnetic tape. A time code derived from the site's cesium-beam clock (with stability of one part in 10^{11}) was also recorded. Portions of the analog taped data were digitized and all subsequent processing was performed on a 16-bit Hewlett-Packard Model 2100 minicomputer.

Further specifications of this array and the various receiving and recording instruments available at WARF can be found in Refs. 3 and 4. Since the wide-sweep backscatter sounding capability was heavily used in support of the current research, it is briefly described in Appendix A of this dissertation.

---

*Modifications just completed at the time of this writing now provide some backlobe suppression.

8727-25-196

FIGURE 1 THE WARF 2.5-km HF RECEIVING ANTENNA

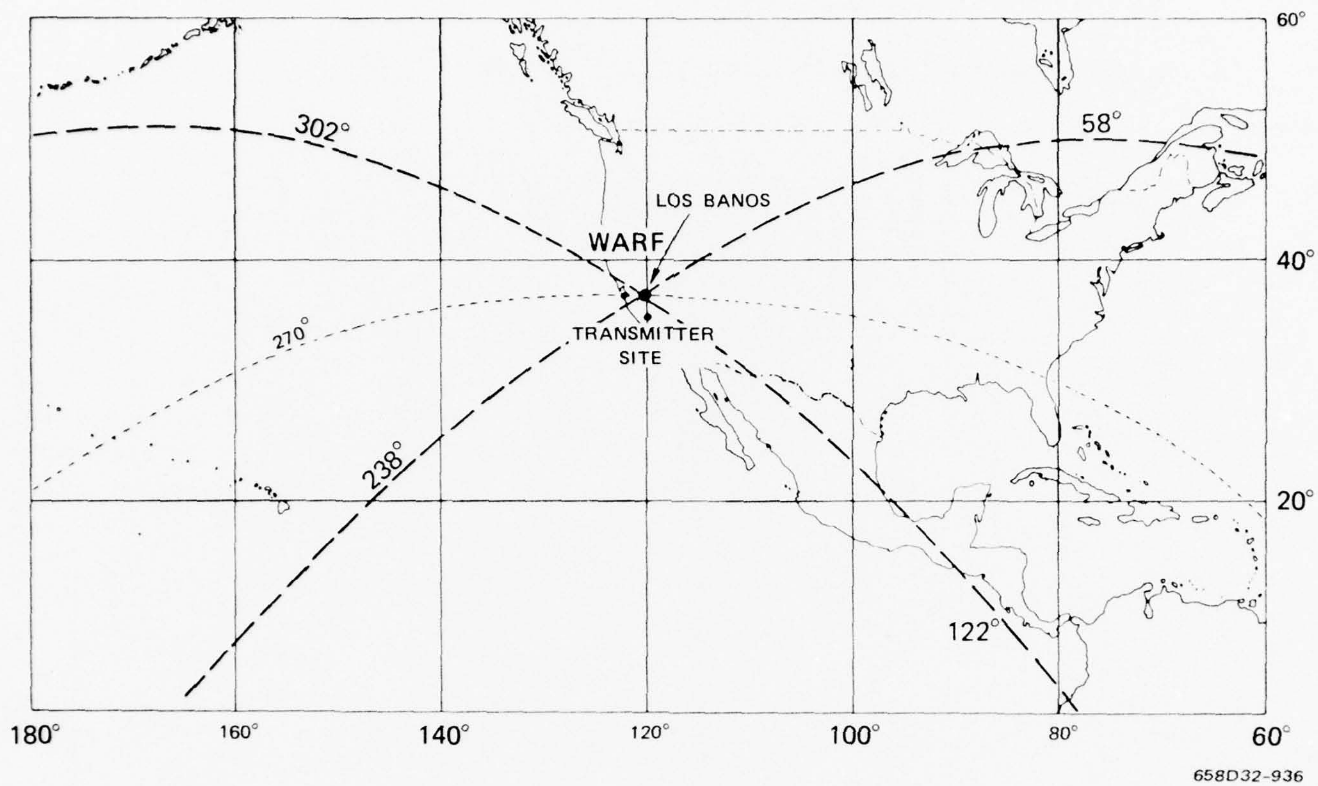

FIGURE 2 WARF ANTENNA STEERING LIMITS

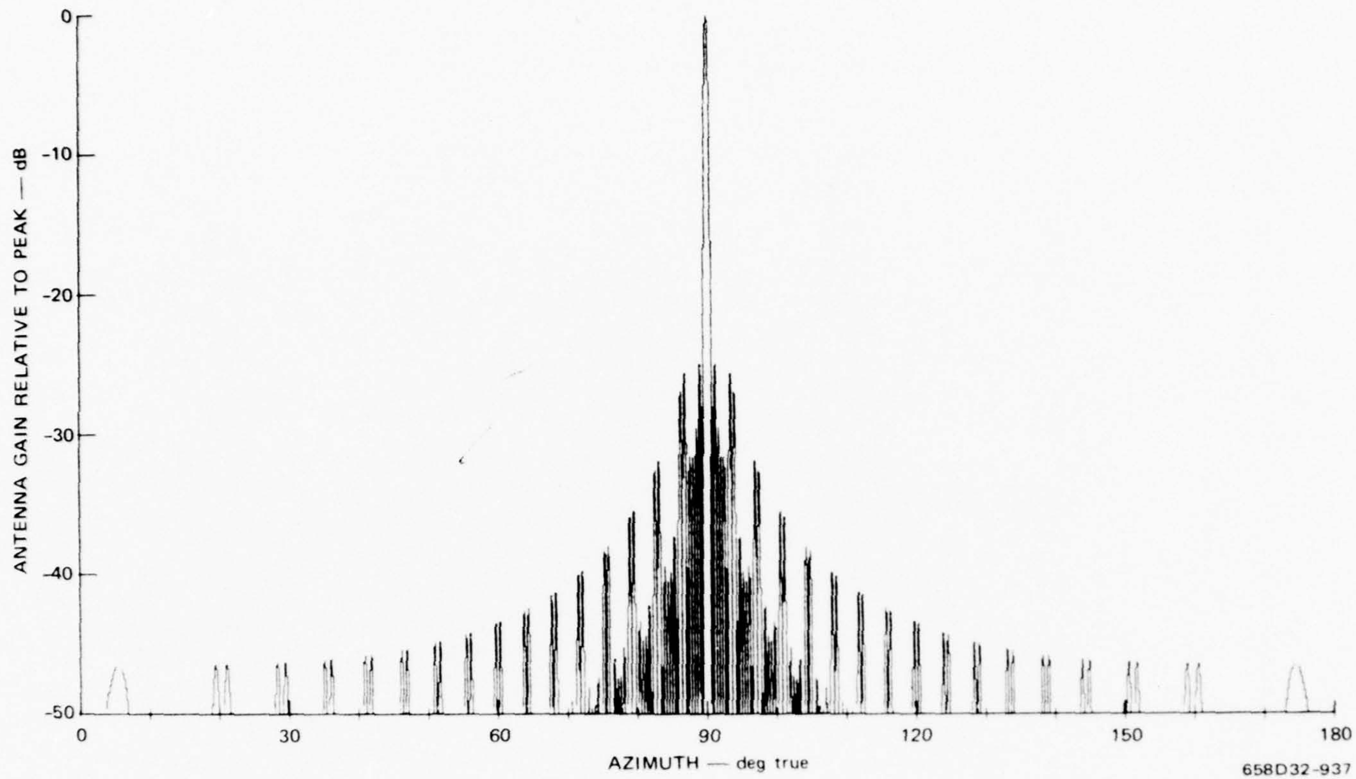

FIGURE 3 ANTENNA PATTERN FOR A 15-MHz FREQUENCY AND A BORESIGHT (90°) STEER

B. Remote Field Site

For simultaneous skywave and line-of-sight recordings of atmospherics, a field site was used in conjunction with the WARF. The field site was deployed to various parts of New Mexico to record atmospherics from close lightning. Field-site equipment consisted of HF and ELF antennas, receivers, and an analog tape recorder. A block diagram of the equipment configuration is shown in Figure 4. The timing standard was synchronized to an accuracy of 20 ms by receiving National Bureau of Standards timing signals from WWV--Boulder, Colorado. Site-to-WARF synchronization of better than 1 ms was later achieved by adjusting the time-base of data received at the remote site so that the first strong atmospheric received at both sites appeared coincident. The rough initial synchronization was sufficient to enable this atmospheric association process to work without ambiguity. The 1-part-in-10^9 stability of the crystal standard used at the remote site ensured that the resulting adjustment was adequate for the remaining data collected during that thunderstorm.

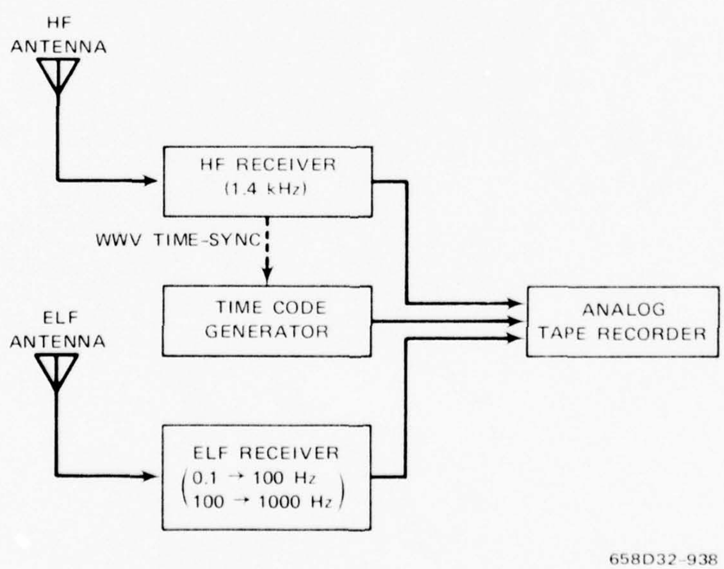

FIGURE 4 BLOCK DIAGRAM OF FIELD-SITE EQUIPMENT CONFIGURATION

The ELF receiving system was of new construction and is worthy of further comment. Its antenna, shown in Figure 5, was reproduced from a design by Barham.[35] The electronics consisted of a preselector filter and amplifier housed at the base of the antenna and a receiver with tuned filters and amplifiers.

The receiver was equipped with two filters of different bandwidths--0.1 to 100 Hz, and 100 to 1000 Hz. While the first was preferable because it responded principally to changes in the electrostatic component of close lightning, it could not be used near commercial power lines. At times when such operations were unavoidable the 100-to-1000-Hz filter was used.

FIGURE 5 VERTICAL ANTENNA USED FOR MEASURING THE ELECTROSTATIC FIELDS OF CLOSE LIGHTNING

III CHARACTERISTICS OF HF ATMOSPHERIC NOISE RECEIVED ON A DIRECTIONAL ANTENNA

To determine if a directional HF antenna such as that at WARF can be a useful tool for observing individual atmospherics of remote origin, it is necessary to investigate the interaction between antenna pattern and atmospheric noise. At HF, non-manmade noise is comprised of cosmic and atmospheric components. While the amplitude and time distributions of cosmic noise approach those of thermal, this is not true for atmospheric noise. And such noise often predominates at frequencies below 20 MHz.

Beckmann[36] explained that HF atmospheric noise approaches a Rayleigh distribution for small amplitudes (and high probabilities). This is presumably caused by the averaging or overlapping of independent atmospherics. For the large amplitudes (and low probabilities) the distribution diverges from Rayleigh, becoming more variable. These large amplitudes are presumably caused by infrequent, strong atmospherics; perhaps from close-by lightning. Crichlow[20] used a geometric construction of two straight lines connected by a circular arc to describe essentially the same cumulative probability distribution. It is significant that the data used in all these analyses were received on omnidirectional antennas.

Horner[1] observed that the properties of atmospheric noise may be dependent on the directivity of the antenna used in their reception. The noise becomes more variable with increasing directivity--being principally controlled by in-beam thunderstorm activity. From this we might postulate that an appropriate model for atmospheric noise received with a directional antenna would be composed of a low-amplitude (high-probability) Rayleigh component caused by the many atmospherics entering through the antenna's sidelobes, and a comparatively high-amplitude (low-probability) component caused by in-beam atmospherics. As long as the storm is beyond the skip distance for the frequency of observation, these in-beam atmospherics need not be close-by as for the case of an omnidirectional antenna. This suggests that for a directional

antenna such as that at WARF, the received noise will have, superimposed on a continuum of weaker Rayleigh noise, strong and commonly nonoverlapping atmospherics preserving enough detail to make useful measurements of remote lightning flashes.

A. Experimental Observations of Noise Characteristics Versus Antenna Directivity

To test the effect of antenna directivity on the characteristics of received HF noise, data were recorded using the 0.5° WARF antenna and an omnidirectional vertical monopole situated about 100 m away. HF noise was simultaneously received on two matched receivers of 1.4 kHz bandwidth. The data were recorded on a summer afternoon when no local storm activity was present. The WARF antenna was pointed in the general direction of known midwestern thunderstorm activity.

Each receiver output was sampled at a 5000-Hz rate. The rms value, E_{rms}, computed over five samples (corresponding to 1 ms) was used to estimate the noise envelope. These 1-ms samples were calculated for a 30-s interval of data and used to construct empirical amplitude-probability distributions. Representative samples of the resulting distributions are shown in Figure 6. These cumulative distributions have been plotted on Rayleigh probability paper, which has the characteristic that a Rayleigh distribution takes the form of a straight line of slope -0.5. The distributions of Figure 6 exhibit low-amplitude Rayleigh components with more variable high-amplitude components in agreement with the distributions observed by Beckmann[36] and Crichlow.[20]

The distributions in Figure 6(a) have been normalized by the rms average of their envelopes in accordance with the conventions used by the authors mentioned above. However, for the purpose of comparing the distributions obtained from different antennas, it is convenient to equalize the common Rayleigh noise "background." This was accomplished in Figure 6(b) by renormalizing the distributions by their respective mode* values.

---

*The mode represents the value for which the amplitude-probability density function attains its maximum.

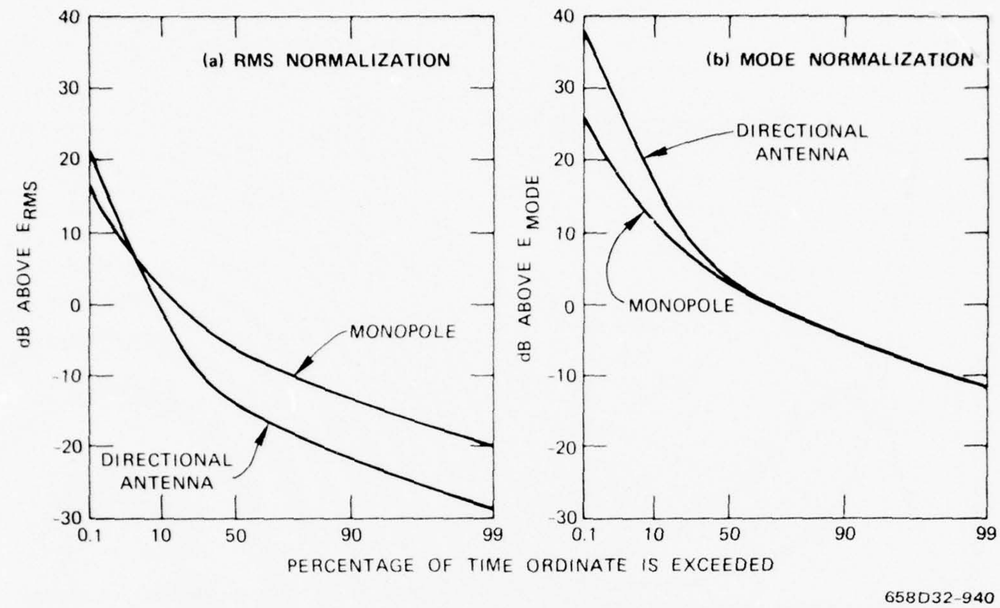

FIGURE 6 CUMULATIVE AMPLITUDE-PROBABILITY DISTRIBUTIONS OF NOISE RECEIVED ON ANTENNAS OF DIFFERENT DIRECTIVITY

In Figure 7 the data of Figure 6 have been replotted as amplitude-probability density functions on a linear scale. This figure demonstrates that the mode is strictly a function of the Rayleigh portion of the distribution. Other statistics such as the rms, mean, and to a lesser extent, median, are dependent on the variable high-amplitude component of these distributions.

From Figure 6(b) it is evident that the high-amplitude component of the observed atmospheric noise is more pronounced for the directional antenna. Review of the data in the time domain is necessary to determine if this component is produced by individual atmospherics. Figure 8 plots one-second intervals of the data used to compute the distributions of Figure 6. The envelope of the noise received with the two different antennas has been normalized by their respective mode values to provide equal noise backgrounds. It can be seen that most of the high-amplitude values are clustered in discrete bursts. Although hardly observable on the monopole data, the time/amplitude characteristics of the noise bursts

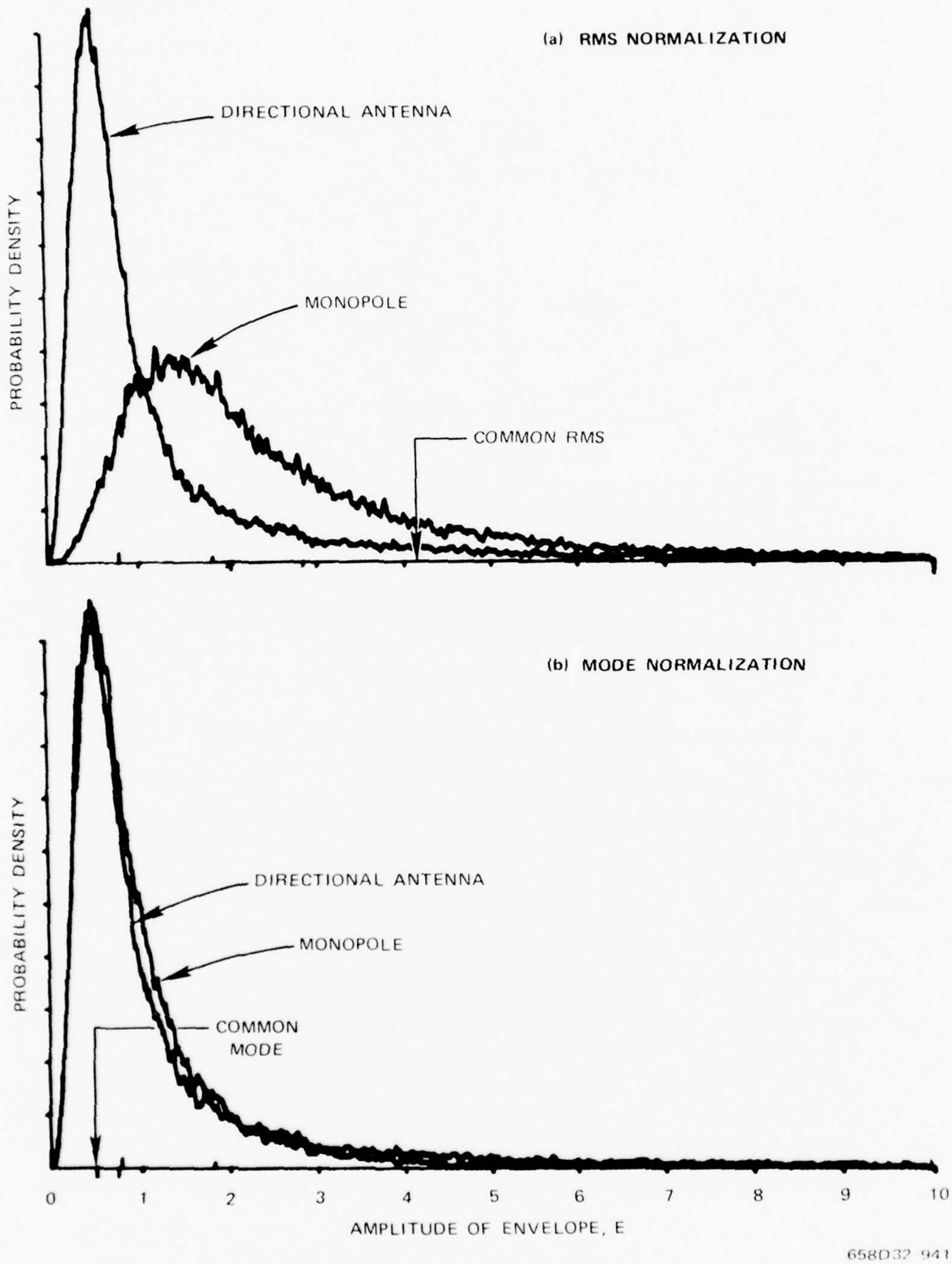

FIGURE 7 AMPLITUDE-PROBABILITY DENSITY DISTRIBUTIONS FOR DATA OF FIGURE 6

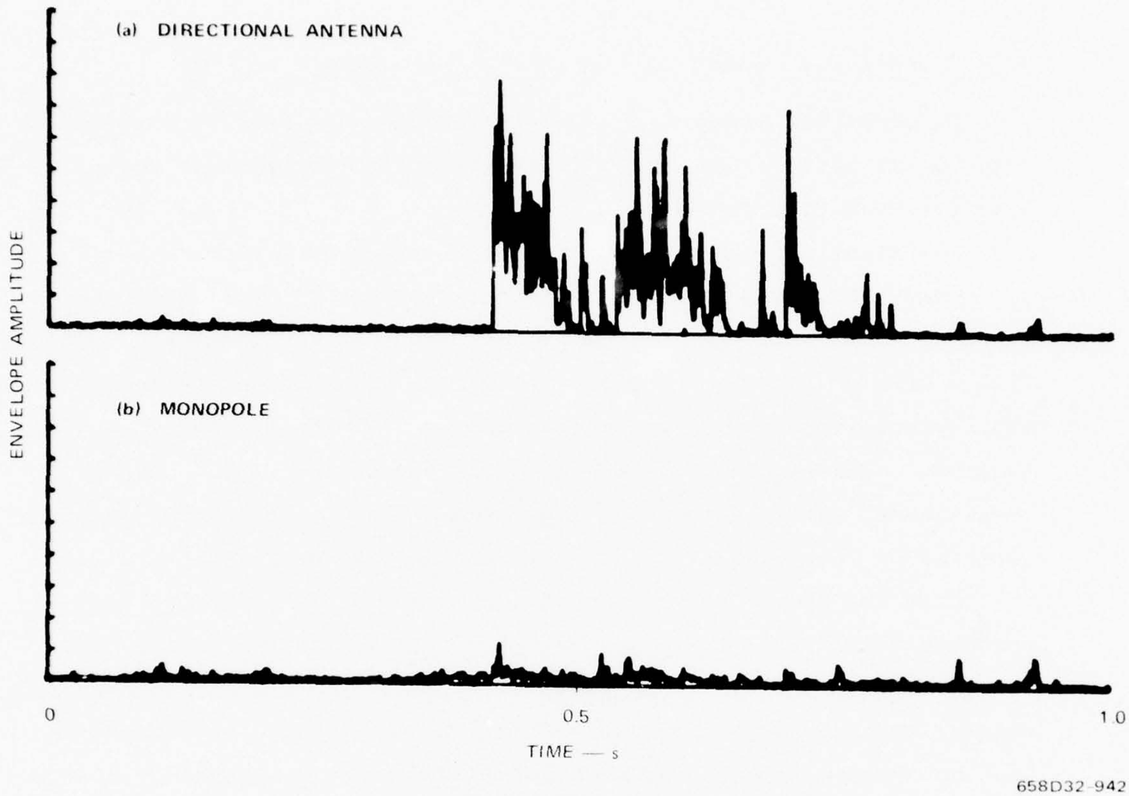

FIGURE 8 ENVELOPE OF RECEIVER OUTPUT vs TIME

received on the directional antenna are similar to observations of single HF atmospherics radiated from close lightning flashes.[16,18] (The receiver passband was too narrow to resolve individual impulses and the atmospheric therefore takes the form of a continuous burst of noise.) Furutsu[22] showed that HF noise distributions with such unusually strong amplitude components can be caused when local thunderstorms are present. But, since no local storms were present, the weight of evidence suggests that these strong atmospherics originated from remote flashes (presumably at a one-hop distance) and were received via skywave propagation.

An indirect method of testing this conclusion was to estimate a likely thunderstorm spatial distribution for one-hop distances from the WARF antenna and determine if the resulting atmospheric noise is comparable to the noise observed.

B. A Model for One-Hop Atmospheric Noise Received at WARF

To construct a model of atmospheric noise incident on the WARF antenna, it is first necessary to describe the thunderstorm activity likely to create that noise.

The flashing rate of a thunderstorm varies over the course of each storm and from storm to storm. Cianos[37] notes that observations of flashing rates have varied from one to more than ten flashes per minute with a mean of three. The duration of each flash also varies with most measurements, showing an average of 500 ms.[37] The atmospheric noise received on an antenna can be modeled, after Ortenburger,[23] as the summation of atmospherics from many storms--each contributing an amount weighted by its propagation path and the antenna pattern.

Near the WARF receiving antenna located in the Central Valley of northern California, there are seldom any local thunderstorms. The Sierra Nevada Mountain Range provides a moderate source of line-of-sight storms, but groundwave losses over this 80-km path are comparable to one-hop skywave losses. As a consequence, the major source of HF atmospheric noise received at WARF propagates via ionospheric reflection. Because of lower path losses, those storms in the midwest having a one-hop propagation path will predominate over storms from the more electrically active tropical regions, which require multiple-hop propagation paths.

Figure 9 shows a representative example of the region having strong one-hop propagation to WARF. This region will change with choice of receiving frequency and ionospheric conditions; however, it is useful for estimating the approximate azimuthal flashing-rate density. To simplify calculations we will assume propagation losses to be constant throughout the one-hop region. The numbers shown in Figure 9* are

---

*The number of ocean thunderstorms is thought to be negligible compared to land storms. Recent WARF antenna modifications provide east-west backlobe discrimination, and initial measurements support the assumption that most atmospheric noise received at WARF originates to the east of the antenna.

FIGURE 9 AVERAGE MONTHLY SUMMERTIME THUNDERSTORM — DAYS WITHIN A TYPICAL ONE-HOP PROPAGATION REGION FROM WARF

derived from the summertime monthly thunderstorm-day statistic.[38] These statistics estimate the number of days per month that thunder is heard at a particular location.

Using a relationship developed by Pierce,[39] we can estimate the flashing-rate density from the thunderstorm-day statistic. If we assume an average of 9 for the summertime monthly thunderstorm-day statistic in the one-hop region of Figure 9, the afternoon flashing-rate density can be estimated at $1.8 \times 10^{-4}/\mathrm{km}^2$-min. Applying this spatial flashing-rate density to the geometry of Figure 9 results in an average azimuthal flashing-rate density of 4.4 flashes per degree-minute. Over the electrically active one-hop-by-60° sector shown in Figure 9 (and ignoring the remaining relatively nonactive one-hop region), this average flashing rate would yield a total of 265 flashes

per minute.* Since each flash lasts several hundred milliseconds, this calculation indicates that radiation from several one-hop flashes may be received simultaneously. Thus, for an omnidirectional antenna the received atmospheric noise will be nearly continuous and atmospherics from individual flashes will not be easily recognized. In contrast, for the 0.5° antenna at WARF, the average in-beam flashing rate is only 2.2 flashes per minute. Because this narrow beam intersects a relatively small area, localized weather conditions make it likely that the actual in-beam flashing rate will substantially deviate from the average. However, even considering an in-beam flashing rate as high as 10 per minute, most flashes will be separated from one another in time. If the antenna gain and sidelobe levels are adequate, these in-beam events should be strong, compared to the continuum noise background produced by the many out-of-beam events.

In conclusion, it should be stated that the above model of HF atmospheric noise incident at WARF must be considered as a very rough approximation. Propagation or localized weather conditions may easily place this model in error by an order of magnitude. However, the calculations are useful in substantiating the preliminary conclusion that the directional antenna at WARF has the capability to observe atmospherics from individual remote lightning flashes.

---

*It is expected that these flashes would not be evenly distributed over such a large area. However, only the total flashing rate, not its azimuthal distribution, is of importance when calculating the atmospheric noise received by an omnidirectional antenna or through the sidelobes of a directional antenna.

IV OBSERVATIONS OF REMOTE HF ATMOSPHERICS

A. Verification of the Source of Atmospherics Observed with the Directional Antenna

The observations described in the previous section imply that many of the strong, and well defined atmospherics received on the WARF antenna originate at a remote distance and then propagate to the antenna via skywave. Direct verification of this hypothesis was made by field measurements. An experiment was designed to record and compare signals received on the 0.5° antenna with measurements simultaneously recorded in the immediate vicinity of a thunderstorm at a one-hop distance from northern California.

1. Design of Experiment

A remote field site was established in an area of New Mexico likely to produce thunderstorm activity. When a storm approached this site, HF noise data were simultaneously recorded there and in California with the 0.5° antenna pointed in the storm's direction. Wide-sweep backscatter soundings were taken at WARF (see Appendix A) to determine the best band of frequencies available for propagation to the remote site and thereby infer, by reciprocity, the best frequency band available from the remote site to WARF. The 1.4-kHz receivers of both sites were then tuned to an interference-free channel within this frequency band. This selection process was principally accomplished by listening to the receiver output for the presence of man-made signals. Simultaneous HF records were then collected at both sites for use in making a comparison of atmospheric noise received via direct and one-hop paths.

ELF records were also recorded at the field site. These records were intended for use in identifying flashes close to the site. The characteristics of ELF radiation from lightning change rapidly with propagation distance.[40] At close ranges the electrostatic field is strong. But this field decreases in proportion to the cube of distance. The weaker radiation field, which decreases linearly with distance, will

predominate at longer ranges. The reception of ELF radiation indicative of a strong electrostatic component can thus be used to identify flashes occurring close to the field site. The simple form of the electrostatic field can also be used to identify specific events within a lightning flash.[40,41]

2. The Remote Field Site

An area in north central New Mexico was selected for the location of the field site. This region was chosen because of its vigorous thunderstorm activity and its good one-hop propagation path back to California. Because the ELF measurement is sensitive to 60-Hz powerline radiation, actual field sites were located several miles from commercial power. The equipment was housed in a van and powered by a gas-driven electric generator. Two New Mexico sites were selected. The first was located near Bernalillo and the second was situated near Redondo Peak in the Jemez Mountain Range.

This experiment was conducted on eleven afternoons during the summer of 1974. Due to unusually dry conditions prevalent in New Mexico, only one thunderstorm--at the start of the first day of operations--came close to either field site. During equipment setup on the afternoon of 31 July 1974 an unusually active thunderstorm developed and slowly passed near the Bernalillo field site. Figure 10 shows a New Mexico radar precipitation map taken at 2230 UT, 31 July 1974. The field site location, and 3-dB and 10-dB footprints of the WARF antenna have been added. While the HF equipment at the field site was not yet operational, good ELF records were obtained. HF noise received with the WARF antenna was simultaneously recorded in California. These data were used to compare noise measurements.

3. Data Comparison

The analog tape recordings from the New Mexico field site were brought back to California and digitized for comparison with the WARF HF records. Figures 11(a) and (c) reproduce ELF measurements

658D32-944

FIGURE 10 FOOTPRINT OF DIRECTIONAL ANTENNA OVERLAID ON WEATHER RADAR PRECIPITATION MAP

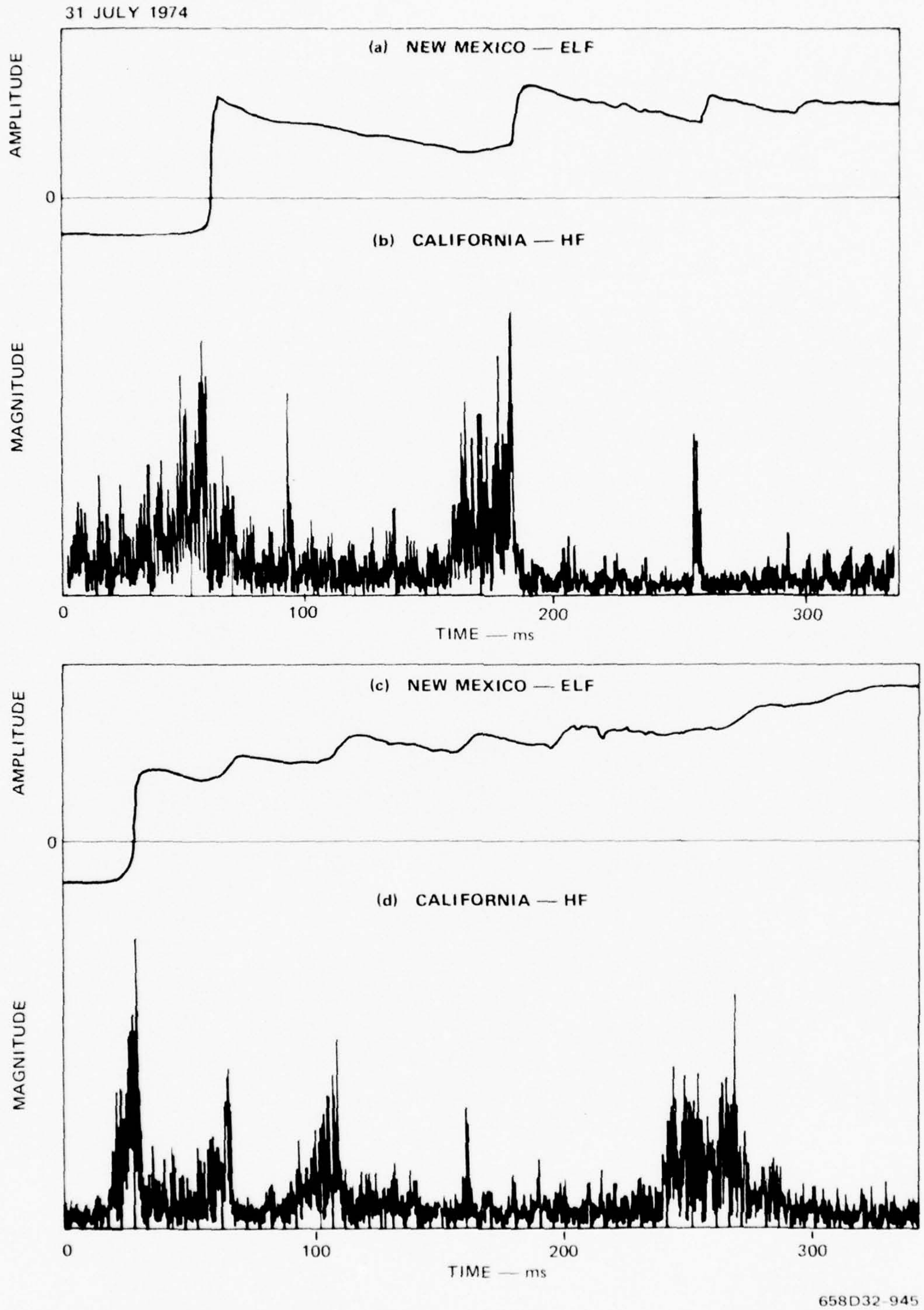

FIGURE 11 ATMOSPHERICS RECORDED SIMULTANEOUSLY IN NEW MEXICO AND CALIFORNIA

recorded in New Mexico. Figures 11(b) and (d), respectively, plot the magnitude of HF noise simultaneously received at WARF. The time axes have been shifted 11 ms to account for differential propagation delays and time synchronization errors as outlined in Section II. This shift has the effect of arbitrarily forcing a correlation between one feature of the first strong atmospheric received at WARF and an equivalent feature received at the New Mexico site. Although the 11-ms shift biased the probability of making this first correlation, results of an analysis described in Appendix B proved that subsequent events were free of bias. As shown in Appendix B, it is extremely unlikely that the observed correlation between features of atmospherics received at both sites could have occurred merely by chance.

Analysis of the ELF records indicate that they were produced by close lightning flashes. The abrupt positive field change is indicative of cloud-to-ground return strokes,[40,41] while the slight positive deflection just prior to the first stroke indicates the initial breakdown and stepped leader phases. A comparison of these ELF records with the HF noise bursts received at WARF shows a high degree of correlation. The HF noise starts with the onset of the breakdown process and increases in amplitude until the return stroke when it abruptly stops for a short period. This quenching of HF noise has been observed in records taken close to cloud-to-ground lightning.[16] It is characteristic of the return stroke and can be used for identification of cloud-to-ground discharges.[42]

Over a 5-minute period, 87% of the flashes recorded in New Mexico were correlated with HF noise received on the WARF antenna in California. For most of these events, the atmospherics received at WARF were sufficiently strong to identify the type of flash and the duration of the initial breakdown process for cloud-to-ground flashes. Radiation prior to the first return stroke of a multiple-stroke cloud-to-ground flash typically produced the strongest signal. Radiation from higher-order strokes was not always observed.

These observations can be made because the effects of ionospheric propagation do little to alter the shape of the received atmospheric. Ionospheric multipath and dispersion will change the shape and number of impulses contained in an atmospheric. However, the 1.4-kHz receiver bandwidth used in this study responds to the envelope of this impulse train, which is insensitive to propagation effects. Other ionospheric effects such as amplitude fading are generally too slow to alter individual atmospherics, which typically last less than one second.

Not all atmospherics received at WARF originated close to the New Mexico field site. Figure 12 plots one minute of received noise on a compressed time scale. Periods when close flashes were recorded on the New Mexico equipment are underlined. The cross-hatched period indicates atmospherics received at WARF and correlated with New Mexico records but also showing evidence of other-event overlap. For the 5-minute interval analyzed, the Bernalillo storms accounted for 35% of the atmospherics received in California. Thunderstorm activity over the California Sierra Nevada mountains and in eastern New Mexico (see Figure 10) most likely caused the remaining atmospherics.

While it was beyond the scope of this experiment to account for all atmospherics, the data directly verified that strong atmospherics of remote origin can be received on a directional antenna. Furthermore, event overlapping is sufficiently reduced that individual atmospherics can be observed and used to identify events within a flash.

B. Variations in the Bearing of Noise Received from a Single Lightning Flash

The previous subsection established that information contained in the amplitude-versus-time waveform of atmospherics can be remotely monitored using a directional antenna. In this subsection we will show that the atmospheric wavefront contains information on horizontal variations of the radiation source involved within a single remote flash. This surprising observation was noted when the WARF was configured to obtain accurate bearing estimates of remote atmospherics.

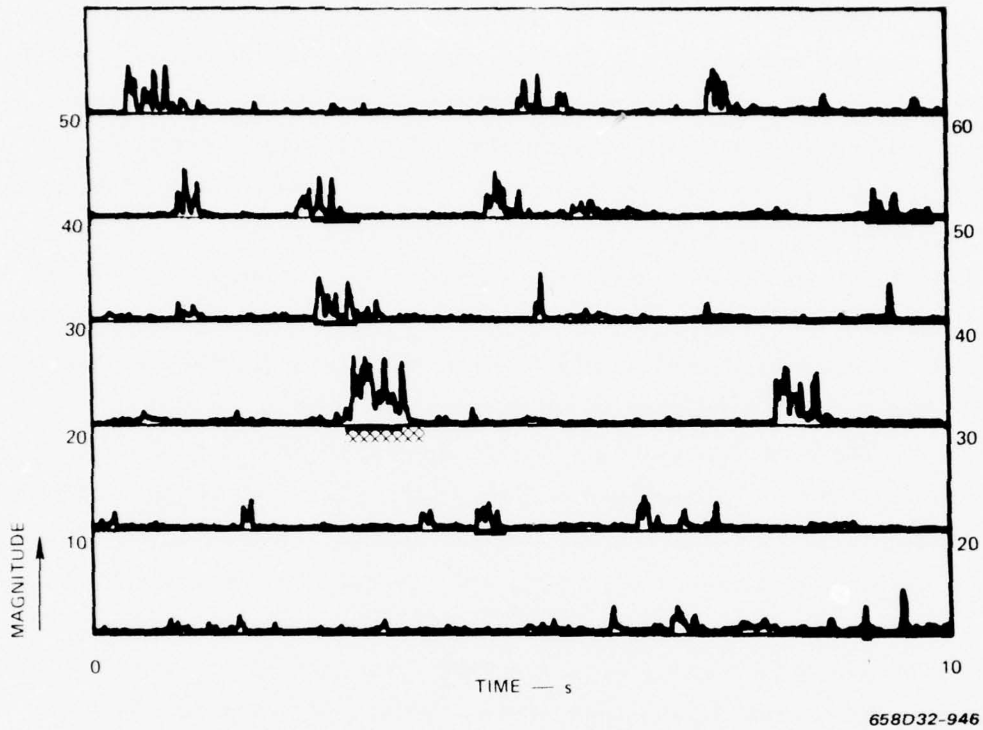

FIGURE 12 ATMOSPHERIC NOISE RECEIVED WITH THE WARF ANTENNA POINTED IN THE DIRECTION OF THE BERNALILLO STORMS

1. Bearing Estimation of Atmospherics

A digital beamforming technique was used with the WARF antenna to produce eight simultaneous 0.5° beams spaced 0.5° apart. This technique is similar to that developed by Sweeney[5] but is simplified by the addition of an eight-channel coherent receiver with matched passbands[43] and eight simultaneous analog-to-digital converters. The 2.5-km antenna is divided into eight equal parts. An analog beam is formed for each of the eight subarrays. Noise from each of these 4° beams is received on one of the eight receiver channels. The outputs are digitized and processed through a two-dimensional Fourier transform to obtain bearing estimates of the received noise. Independent bearing measurements are computed for every 4 ms of data. (Further details of this digital beamforming technique appear in Appendix C.)

When eight contiguous beams are formed simultaneously, the received noise energy versus azimuth and time can be computed. While azimuthal resolution is fixed by antenna length, single-source azimuthal accuracy is limited only by SNR. For skywave propagation, absolute accuracy is further limited by coning errors and by deviations from great-circle propagation due to ionospheric tilts. These factors do not affect relative azimuthal accuracy (i.e., measurements of azimuth difference). With adequate SNR, interpolation can be used on the digital beamformed output to measure the relative azimuth-versus-time structure of an atmospheric to an accuracy of 0.06°.

The beamformer output can be described with the aid of Figure 13. The noise received on one of the eight subarrays is plotted in Figure 13(a) in magnitude-versus-time format. Figure 13(b) plots these data as beamformed noise-magnitude versus time and azimuth in a pseudo-three-dimensional format. The atmospheric shown in Figure 13 was recorded on 10 April 1975. Its origin is unknown but was probably a storm system over eastern New Mexico and the Texas panhandle. The azimuthal variation of this atmospheric was confined to within a 0.15° sector.

2. Observations of Azimuthal Variations

Figure 14 plots the amplitude versus time and azimuth of a record containing an atmospheric recorded roughly 20 minutes after that of Figure 13. During the 700 ms of this burst, the apparent direction of arrival changes by 0.7°. Analysis of ten atmospherics received on 10 April shows an average azimuthal variation of $0.5^{\circ} \pm 0.2^{\circ}$.

A horizontal variation in the electrically active cloud region during a lightning flash is one plausible explanation of these observations. Work by Ogowa,[44] Proctor,[45] and Few[46] have recently shown that the in-cloud charge region involved during a flash commonly has a larger horizontal component than was previously assumed. Because the range to the origin of the 10 April atmospherics was unknown, the cross-range distance corresponding to the observed azimuthal change

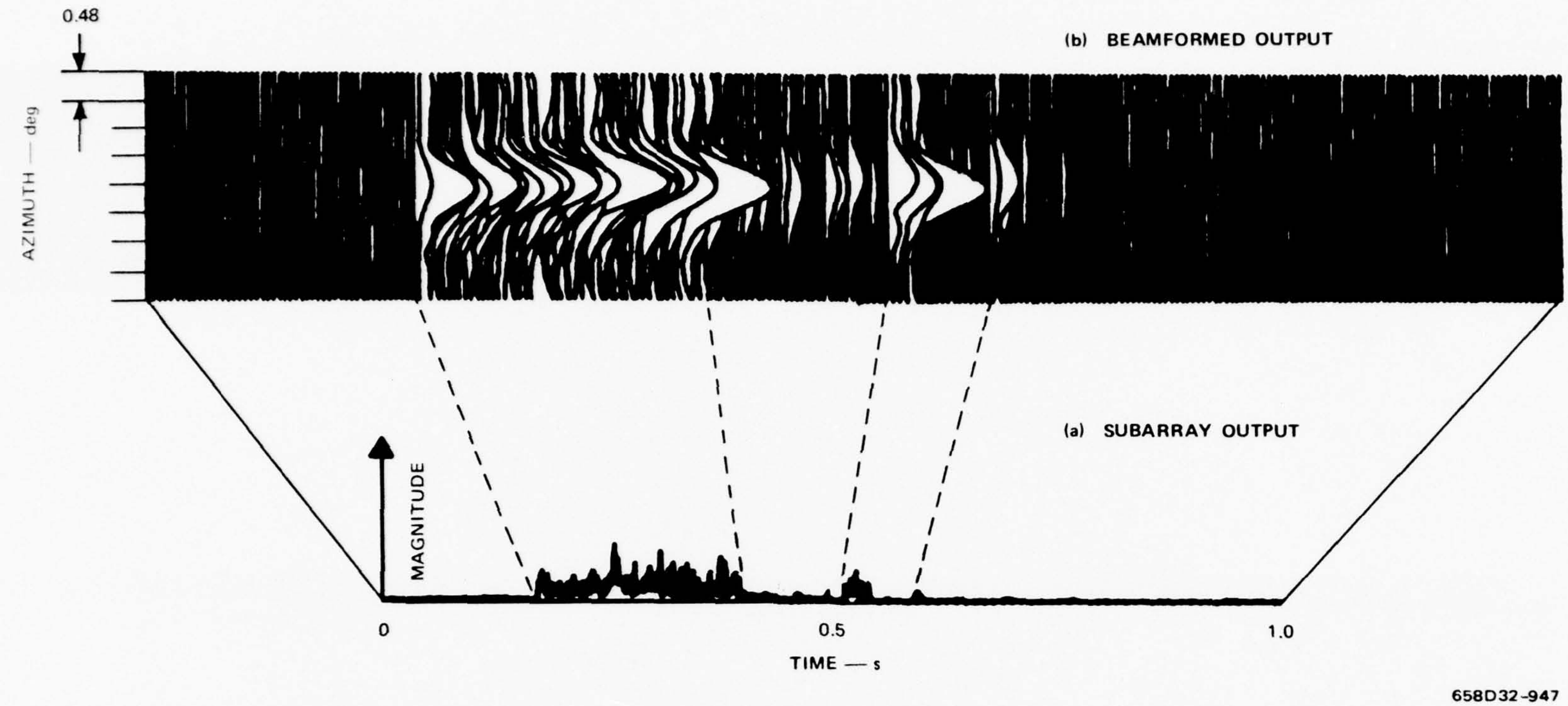

FIGURE 13 AN EXAMPLE OF AN ATMOSPHERIC HAVING A SMALL VARIATION IN ITS DIRECTION OF ARRIVAL

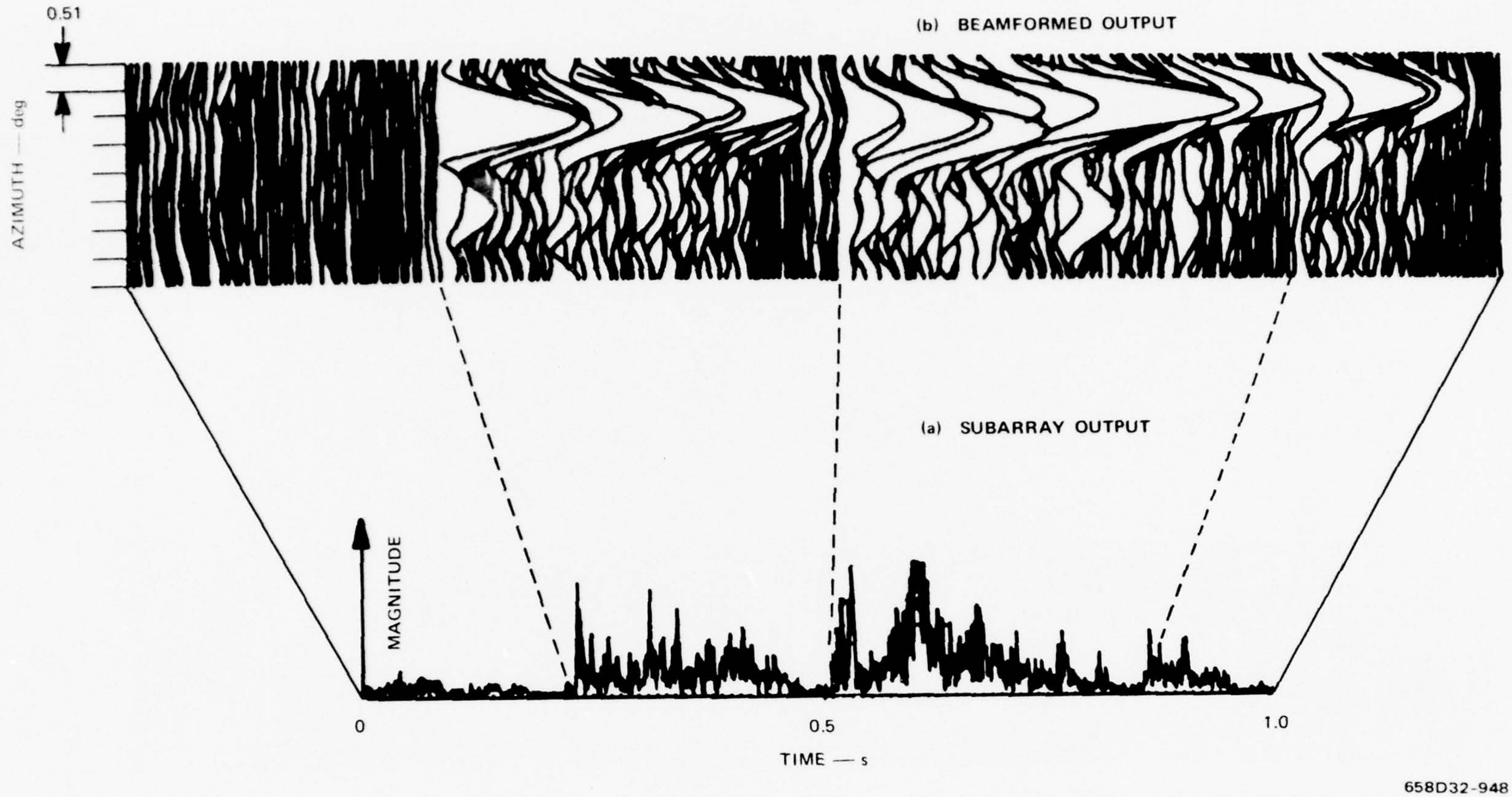

FIGURE 14 AN EXAMPLE OF AN ATMOSPHERIC HAVING A LARGE VARIATION IN ITS DIRECTION OF ARRIVAL

can only be estimated.* Without direct verification, the possibility of equipment malfunction or ionospheric propagation peculiarities must be considered before presuming that these observations were actually the result of changes within the flash. A second New Mexico field test ruled out the possibility of these alternative explanations.

During July of 1975 a field site in Los Lunas, New Mexico was manned for an unrelated experiment. The HF and ELF receiving equipment used in the field experiment described in the previous section was installed and at the ready if a thunderstorm should occur close by. Because of the proximity to power lines, the 100-to-1000-Hz ELF passband was used. On 10 July 1975 a thunderstorm passed close to the Los Lunas site. Data from this storm were simultaneously recorded in New Mexico and at WARF.

Changes in the received azimuth of a single atmospheric were again observed on 10 July. Figure 15 shows a one-second record of the Los Lunas ELF (a) and HF (b) channels along with the subarray (c) and beamformed (d) data received simultaneously at WARF. The horizontal line through Figure 15(d) indicates the observed bearing of a calibration signal received at WARF and transmitted from Los Lunas. During the one second of data displayed in Figure 15, noise from two flashes was received with the WARF antenna. The first flash evidently originated from a storm other than the one over Los Lunas. This is concluded because noise from this flash was not received in Los Lunas and the observed azimuth was 0.84^{o} away from the Los Lunas bearing. In contrast, the second flash appears to have come from the Los Lunas storm. The received noise from this flash shows a total bearing change of 0.52^{o} over 120 ms for an average cross-range rate of $4.3^{o}/s$.

---

*Based on the propagation conditions observed on the wide-sweep backscatter soundings, atmospherics from storms between 950 and 1600 km might have been received. Weather Bureau data show only one storm system within this area. The range to this storm was approximately 1500 km, suggesting an average cross-range variation of 13 km.

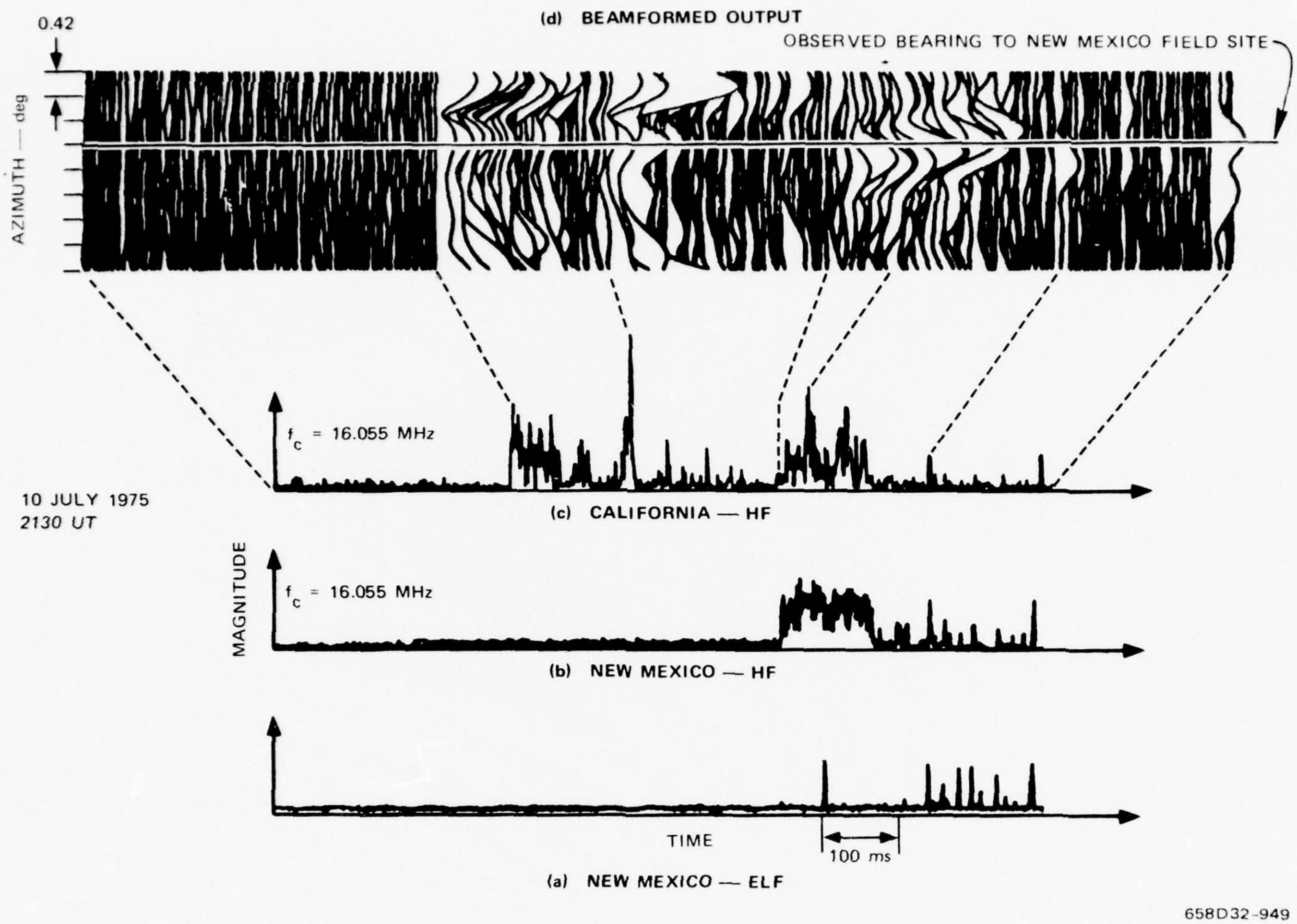

FIGURE 15 DIRECTION-OF-ARRIVAL VARIATIONS FROM AN ATMOSPHERIC ORIGINATING OVER LOS LUNAS NEW MEXICO (1340 km from receiver)

During data collection from this storm a signal was periodically transmitted from the Los Lunas site and received at WARF. The amplitude versus azimuth and time of this signal was computed by the same beamforming program. A 0.24^{o} azimuthal variation of this reference signal was observed over 27 s with a maximum rate of $0.04^{o}/s$. This is two orders of magnitude smaller than the rate observed in the atmospheric of Figure 15.

The reference signal propagated via essentially the same ionospheric path and was received and processed in the same way as atmospherics received from the storm. Since azimuthal fluctuations in the calibrate signal are hardly detectable on a one-second time scale, it can be assumed that neither equipment nor ionospheric effects can explain the apparent directional changes observed in some atmospherics.

The azimuthal extent of 33 flashes determined to have originated in the Los Lunas storm were analyzed. Using 1340 km as the slant-range distance between the WARF antenna and Los Lunas (appropriate for the E_s propagation conditions present), the cross ranges corresponding to the measured azimuthal changes are plotted in Figure 16. On the average, these values are larger than the 3 to 8 km measured by Proctor[45] (at VHF) and Ogawa[44] (at ELF). On the other hand, the distribution of lengths is remarkably similar to those measured by Few[46] (using acoustic signals) for frontal type thunderstorms. It should be emphasized that the various results cited here were obtained using different measurement techniques and hence are sensitive to different processes within the flash.

In summary, observations of atmospherics described here show substantial changes in direction of arrival, which were not observed on a ground-based calibration source. While the elevated geometry of the lightning radiation might account for minor differences, it is not a likely explanation for the substantial differences observed between the azimuthal characteristics of these two signal sources. Although it has not been confirmed by direct measurements, the data provide strong evidence that the measured direction of arrival of remote HF

atmospherics is influenced by spatial properties of lightning processes. Line-of-sight measurements, such as those developed by Ogawa, Proctor, or Few, made simultaneously with remote HF measurements would be useful for studying the relationship between the geometry of the lightning process and the direction of arrival of its remotely received atmospherics.

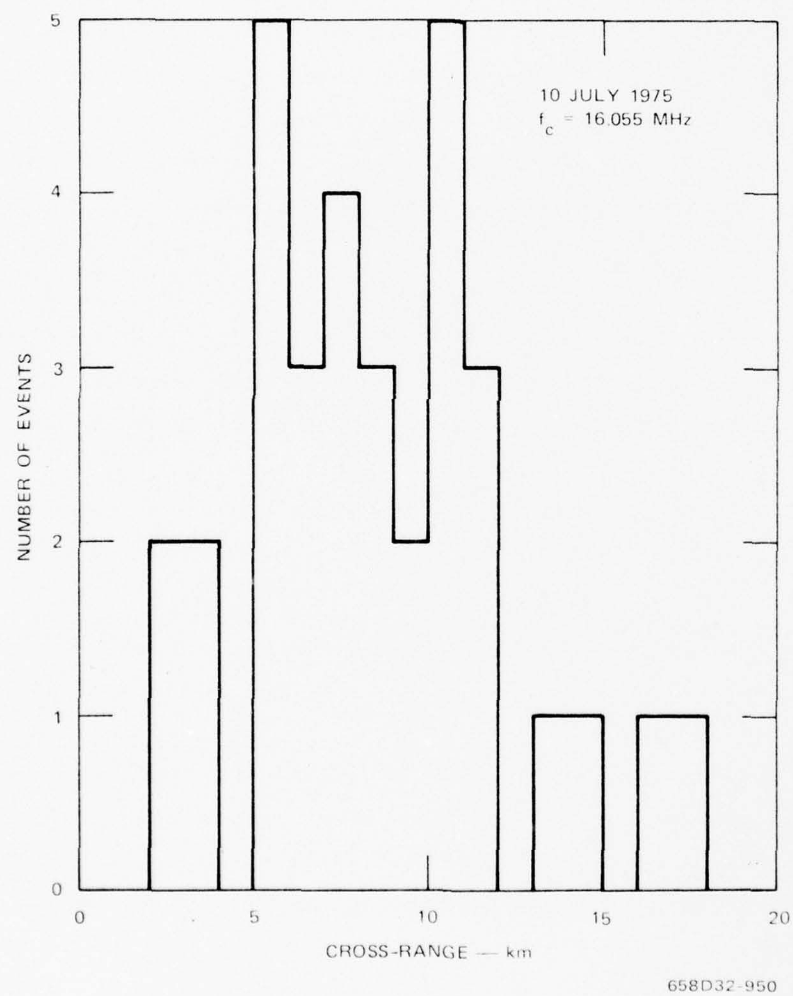

FIGURE 16 DISTRIBUTION OF THE MEASURED HORIZONTAL EXTENT OF LIGHTNING FLASHES ORIGINATING OVER LOS LUNAS, NEW MEXICO

V INVESTIGATION OF HF ATMOSPHERICS FROM SEVERE THUNDERSTORMS

Experiments described in the previous sections demonstrated the ability of a directional HF antenna to observe temporal and spatial properties of individual remote lightning flashes through the reception of the atmospherics they radiate. This capability was applied to observations of atmospherics from remote severe thunderstorms. Over the past two decades researchers have noted that severe storms are usually accompanied by increased electrical activity. Increased radiation of atmospherics during severe thunderstorms has been observed at frequencies between VLF[25,26] and UHF,[30] with recent work concentrating in the HF band.[33,34] However, the author is unaware of any attempt, prior to the work described here, to use atmospherics to study severe storms from ranges beyond line of sight.

In the case of line-of-sight measurements, where the spreading loss of the radiation field predominates, amplitude threshold levels can be set so that only close-by HF atmospherics will be counted. For this reason the total count of atmospherics can be used for sensing the presence of local severe thunderstorms. However, for remote measurements it is possible that several thunderstorms not associated with the severe storm may also lie within the antenna's main beam. In this case the total count of received atmospherics would not be a sensitive measure of the severity of any one storm. Thus for the remote study of severe thunderstorms to be possible, the storms must radiate atmospherics that can be uniquely identified despite the presence of extraneous atmospherics. This section describes an experiment conducted to determine if such a class of identifiable severe storm atmospherics exist. Initial positive indications are presented. The next section will describe a statistical analysis of the observed effect.

A. Experimental Configuration

Clearly, for the study of remote severe thunderstorms via HF atmospherics, data must be collected with an antenna pointed in the

direction of such a storm. But the precise time and location of severe thunderstorms cannot be predicted. Their occurrence is highly sporadic and widely dispersed geographically--even during the springtime peak of the tornado season. Furthermore, severe storms are seen only through their more observable manifestations (e.g., tornadoes, large hail, etc.), and the brevity of these events (the average lifetime of a tornado is 15 minutes)[47] coupled with the delays inherent in current warning procedures make it impractical to gather useful data using reports of sightings.

An alternative to pointing the antenna in the direction of a known severe storm is to scan the antenna over a series of bearings likely to contain such activity. In this way the noise originating within a sizable region can be recorded. Later, the data can be analyzed to discover possible effects caused by storms with severe events sighted in that region. As with any scanning antenna, the larger the azimuth sector scanned, the less time noise is received from any one direction. If a reasonable duty factor is to be maintained, the size of the sector monitored must be limited. This was accomplished by using National Weather Service severe-weather forecasts[48,49] to select those regions within the country most likely to contain severe storm activity.

The National Severe Storms Forecast Center (NSSFC) forecasts areas likely to develop severe thunderstorms. They issue a "Severe Storm Watch" to identify a specific region (nominally 140 miles by 200 miles) and time period during which tornadoes are likely to occur. The location of these regions may vary widely from day to day or even during the course of one day. By the use of these watches the antenna scan sector can be limited while a reasonable probability is maintained of receiving noise from the direction of a severe thunderstorm.

The antenna scanning formats chosen for this experiment represent a compromise among revisit time (the time between successive looks in the same direction), dwell time (the time during which data are received from one direction), azimuthal step size (bearing difference between successive beam positions), and azimuth coverage (total azimuth sector scanned). A five-minute revisit time was deemed the maximum

allowable, considering the brevity of some severe storm events. Thirty seconds was considered the minimum dwell time for evaluation of the received noise structure. Since most severe storm watches occupy an azimuth sector from 10° to 20°, the above constraints lead to a 2° choice of antenna step size. Table 1 describes the resulting two scanning formats used for this experiment. Selection between these two formats depended on current watch information.

Table 1

ANTENNA SCAN FORMATS

	Format A	Format B
Revisit time	5 min	5 min
Dwell time	60 s	30 s
Azimuth step size	2°	2°
Azimuth coverage	8°	18°

Severe storm watches were communicated to the WARF from the Naval Weather Station at Moffett Field and from the San Francisco branch of the National Weather Service. At WARF the watch area was plotted on a U.S. map overlayed with a grid of antenna bearings and approximate one-hop F-layer propagation time delays. An example is reproduced in Figure 17. The watch area is principally contained within a 10° sector, and thus Format A of Table 1 was selected with bearing limits of 100° and 108°. With the use of wide-sweep backscatter soundings, a radio frequency appropriate for receiving noise from the watch area was selected by the technique described in Appendix A. The selected frequency was changed from time to time as ionospheric propagation and man-made interference conditions changed.

B. Data Recording and Monitoring

As the antenna stepped across the scan sector, the noise output from the 1.4-kHz receiver was analog tape recorded along with the

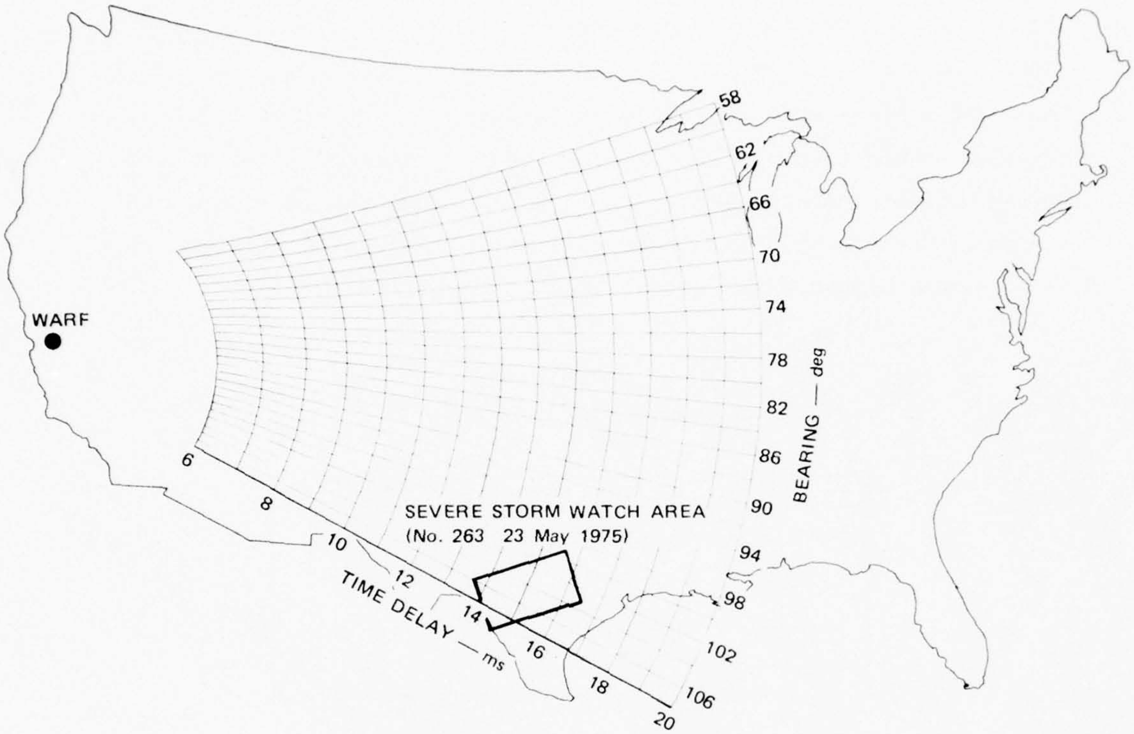

FIGURE 17 A. U.S. MAP SHOWING A SEVERE STORM WATCH AREA AND A WARF DIRECTION/TIME-DELAY OVERLAY

wide-sweep backscatter soundings and a time code. Data were collected in this fashion on several afternoons in the latter half of May 1975. During data collection the noise channel was connected to a speaker and continually monitored by ear. The frequency spectrum of the receiver output was also plotted to provide a continuous hard copy of the received data. These outputs were convenient for monitoring overall atmospheric noise activity as well as weak interference.

This real-time spectral record was obtained by passing the receiver output through a Federal Scientific hybrid spectrum analyzer and outputting the results on an ITT facsimile recorder. The analyzer applies Hanning[50] weights to the incoming data and processes a 0-to-2-kHz bandwidth to 4-Hz resolution. Figure 18 shows two short

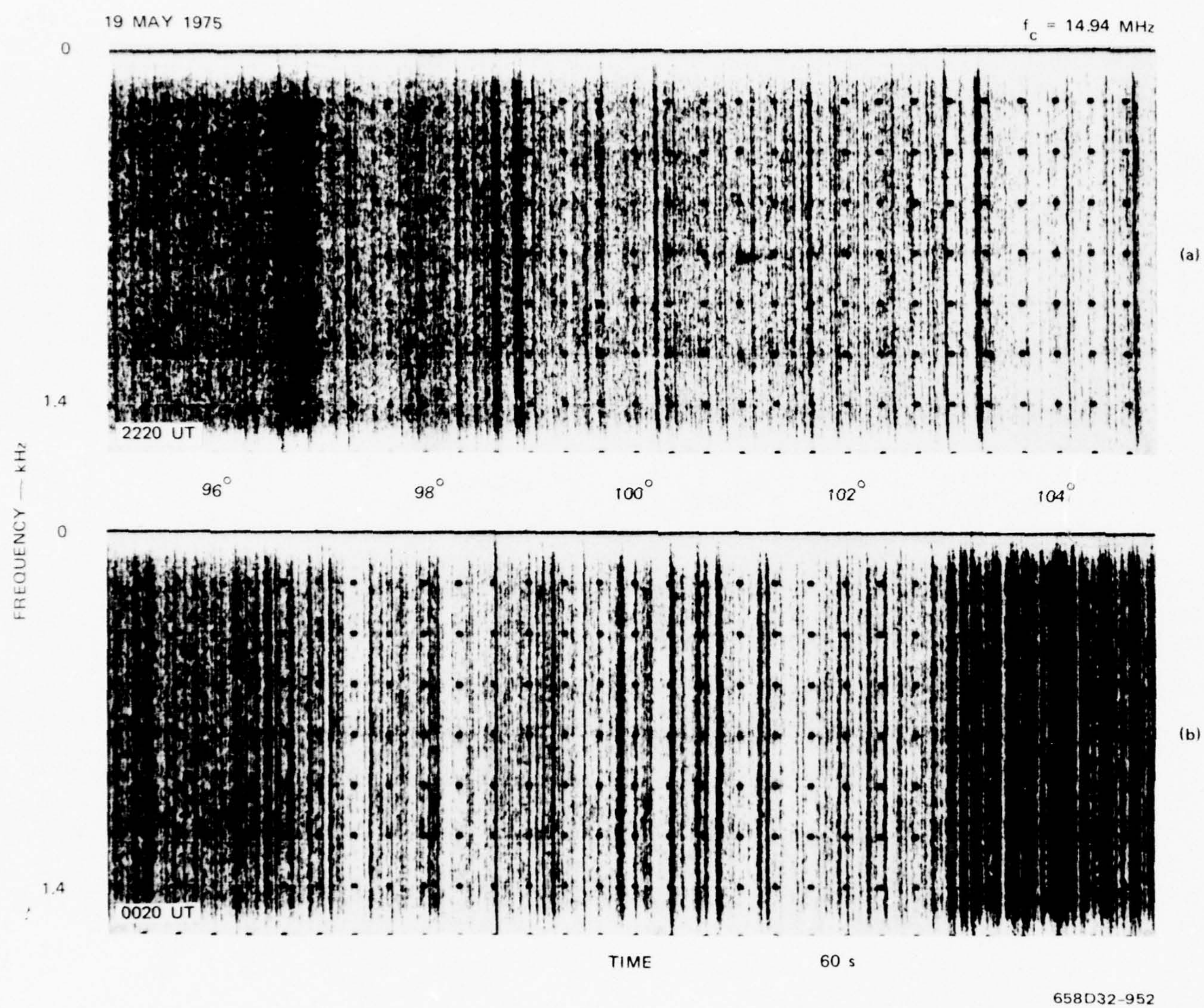

FIGURE 18 PLOTS OF RECEIVED HF NOISE SPECTRA

sequences recorded this way. Receiver IF frequency is plotted versus time (and hence azimuth) with amplitude coded as intensity. Vertical lines are indicative of strong bursts of white noise--presumably from lightning. Horizontal lines would be indicative of spectrally pure signals indicating the presence of some types of interference.

The records of Figure 18 show two five-minute periods spaced two hours apart. During each period the antenna was stepped across the same 8^{o} using scanning Format A of Table 1. The spectral display was useful for estimating the relative amount of thunderstorm activity versus antenna bearing. For example, in Figure 18(a), the northern bearings are the most active. In contrast, two hours later [Figure 18(b)] the southern bearings have become extremely active. As we shall see, this later activity correlates in time and direction to a known severe thunderstorm. But as previously described, the observation of high atmospheric noise activity alone cannot provide a reliable indication of remote severe thunderstorms. For this reason the collected data were next analyzed for a class of HF atmospherics that might be uniquely characteristic of severe thunderstorms.

C. Initial Observations of an Identifiable Class of HF Atmospherics Associated with Severe Thunderstorms

Each day the National Severe Storms Forecast Center compiles a log noting the positions and times of all severe storm sightings. These logs were obtained for days when experimental data had been collected. Initial analysis consisted of reviewing data recorded in the direction of sighted tornadoes. The amplitude-versus-time waveform was carefully reviewed on an oscilloscope. As with the real-time spectral records, this review could easily discern the relative level of storm activity versus antenna bearing. More importantly, at times and bearings coincident with reported severe storm manifestations an unusual amount of isolated noise impulses was observed. This was the first indication of a class of atmospherics having a remotely observable characteristic that could be uniquely correlated with tornadoes and possibly other remote severe storm events.

As described in Section I, HF noise from lightning is characterized by many impulses (each lasting only microseconds) radiating for periods of ten to hundreds of milliseconds. For communication receiver bandwidths (such as those used in this experiment), individual impulses are not resolved and the atmospheric appears as a quasi-continuous "burst" of noise. This is the type of in-beam atmospheric commonly observed with the WARF antenna. While the time/amplitude details of each burst differ, they seldom last less than 10 ms. Thus the observation of many shorter impulses cannot be explained on the basis of normal, even active thunderstorm activity.

Initially, data collected on 19 May 1975 were digitized for further analysis. Several 10-s records from these data are plotted in Figure 19. In each record, 1-ms samples of received noise magnitude are plotted versus time. One second of data appears on each line with subsequent seconds plotted one above the next. The three 10-s records of Figure 19 were taken at the times and bearings noted. Figure 19(b) was recorded at the time and in the direction of a tornado sighted near San Antonio, Texas (a distance of 2200 km from the WARF antenna). The other two records were recorded at times or in directions not associated with reported tornado activity. In all three records, atmospherics characteristic of normal lightning can be observed. Superimposed on this background the record of Figure 19(b) contains a large number of isolated impulses. While Figures 19(a) and (c) contain some impulses, the number and amplitudes of those in 19(b) are significantly higher. Based on this observation, a study was conducted to determine the impulse content of the recorded noise.

D. A Computer Algorithm for Counting Isolated Impulses

To measure the impulse content of atmospheric noise on a large data set it was necessary to devise some automated impulse-counting algorithm. An algorithm employing a fixed threshold would count all noise bursts and the measurement would be dominated by the longer atmospherics possibly originating from normal in-beam thunderstorms. Thus,

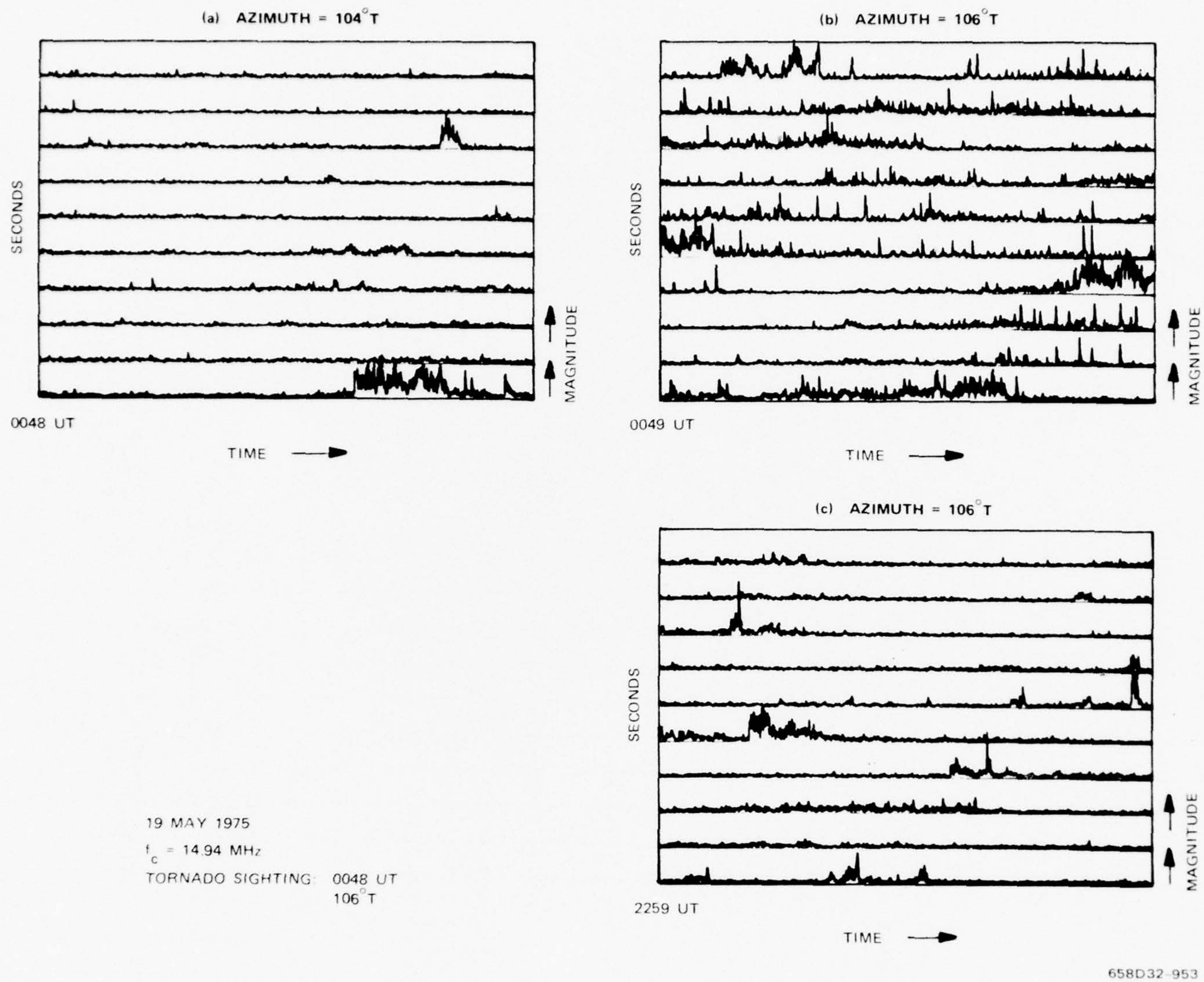

FIGURE 19 AN EXAMPLE OF HF ATMOSPHERICS INDICATIVE OF A SEVERE STORM

any counting algorithm developed must be able to count isolated impulses (presumed to originate uniquely within severe storms) while ignoring those bursts lasting several milliseconds or more (likely to originate within normal storms). By normalization of each 1-ms data sample by a short-term (10 to 50 ms) estimate of its surrounding noise level, a constant threshold algorithm was devised to count only isolated impulses.

Strong noise samples from normal lightning flashes are surrounded in time by other strong noise samples. For this reason the short-term average noise level is high and a sample normalized by this average is not likely to exceed a preselected threshold. For isolated impulses, the surrounding average noise level is low and the normalized sample is likely to be counted.

Figure 20 shows the effect of this impulse-counting algorithm. A 1-s record of noise is shown in Figure 20(a). Figure 20(b) plots the short-term (20 ms) running noise average. Figure 20(c) replots the noise of Figure 20(a) but normalized by the appropriate value of 20(b). Also drawn is a constant 12-dB threshold. Note that the only points to exceed the threshold are from isolated impulses. The algorithm effectively discriminated against the strong and prolonged atmospheric at the end of this record.

The data of 19 May 1975 were used to test various choices of averaging time and threshold in an attempt to optimize the algorithm's immunity to bursts while remaining sensitive to impulses. Averaging times between 10 and 50 ms worked well, while shorter times contained too many spurious counts from normal lightning, and longer times tended to miss too many isolated impulses. Threshold values between 6 and 20 dB were also tried. As the threshold was increased, the number of impulses counted decreased. However, all such counts decreased proportionally, leaving the relative count of impulses roughly unchanged. Thus the algorithm proved insensitive to choices of parameters over a substantial range of values. A 20-ms averaging period and a 12-dB threshold were selected for analyzing the full data set. Results are presented in the next section.

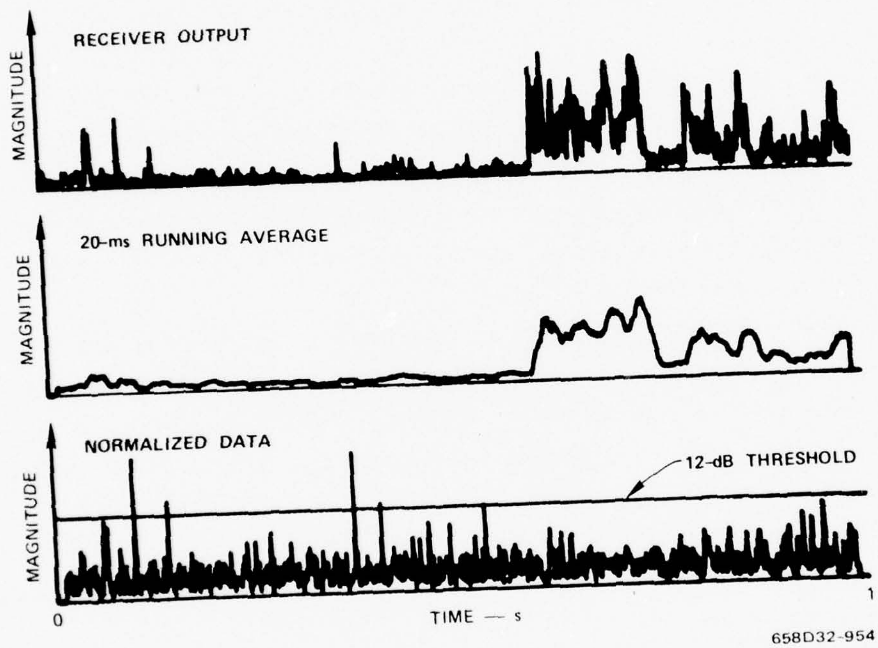

FIGURE 20 FEATURES OF THE IMPULSE-COUNTING ALGORITHM

VI HF IMPULSIVE NOISE CORRELATED WITH REMOTE SEVERE THUNDERSTORMS

In this section, results of the impulse-counting algorithm are compared with reported sightings of severe thunderstorm events. Data collected on the first day of the experiment, 19 May 1975, are presented in detail. Test results from other days are also summarized. The outcome of a statistical test performed to verify the observed correlation is described. Finally, the validity of procedures and assumptions used to formulate the statistical test is discussed.

A. Analysis of Data Collected on 19 May 1975

The numbered dots in Figure 21 indicate locations of tornadoes sighted in the vicinity of San Antonio, Texas on 19 May 1975. Data collected at WARF on that afternoon were processed by the counting algorithm described in the previous section. The results are plotted in Figure 22. Pulse counts are plotted versus time for each of the five antenna bearings. Times of the sighted tornadoes are indicated on the baseline of the closest bearing. The numbers correspond to those of Figure 21. A strong correlation between high impulse counts and tornado sightings is evident. In general, as the storm activity increased, the impulse count increased, reaching local maxima near the sighting times. At the time these data were collected, this unusual impulsive noise component had not yet been associated with tornado activity. In the absence of current weather information, data collection was unfortunately terminated during the height of storm activity.

During the period from approximately 2225 UT until 2300 UT, high impulse counts were observed from the bearing of 102°T. No tornado activity was sighted at that bearing. Three possible explanations can be proposed for this conflicting observation:

(1) These high-impulse counts represent a "false alarm" caused by random noise, interference, or atmospherics from normal storms.

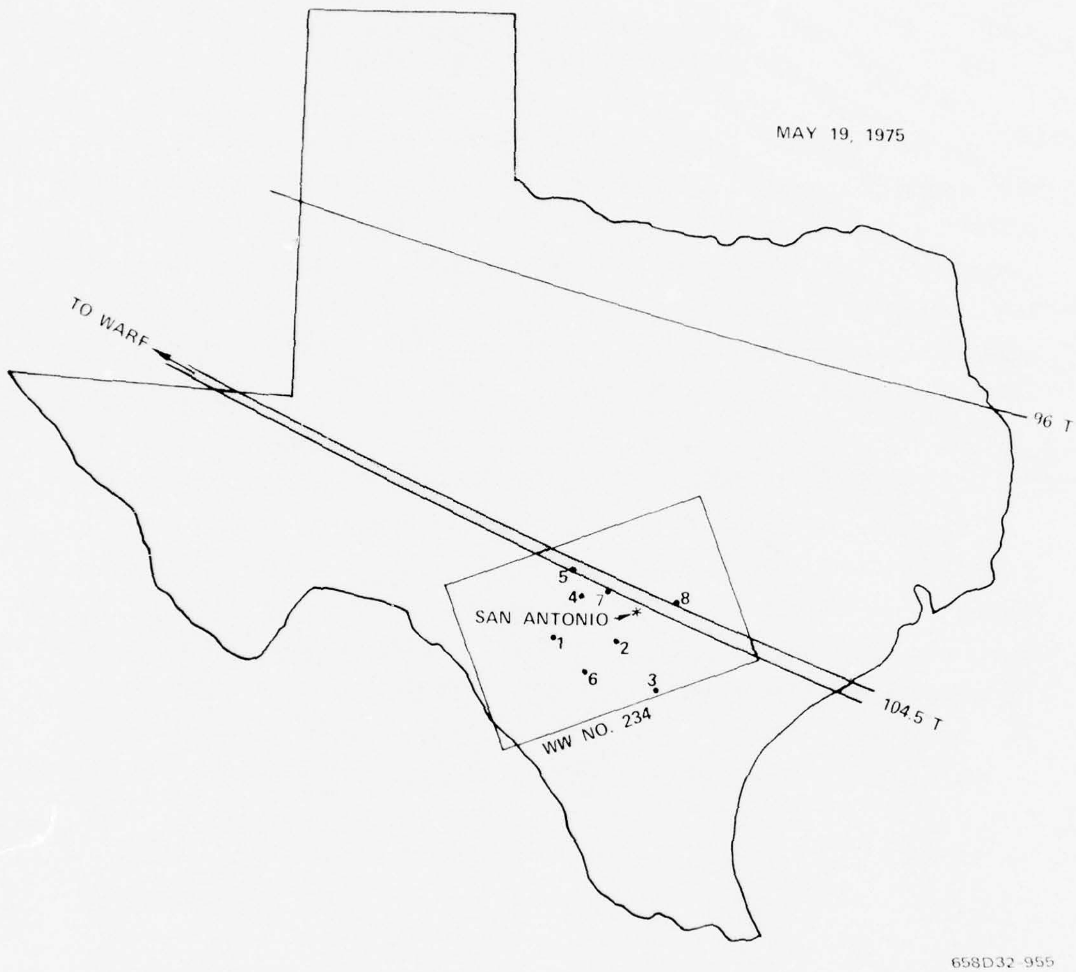

FIGURE 21 WARF ANTENNA SCAN SECTOR IN RELATION TO TEXAS SEVERE STORM SIGHTINGS

(2) The WARF observations correctly indicated the presence of a severe storm, but no observable manifestations were sighted in the vicinity of the storm.

(3) The impulses originated from the severe thunderstorm that spawned the tornado at Location 1 in Figures 21 and 22 (matched in time but off 4° in azimuth) and were received via a close-in sidelobe.

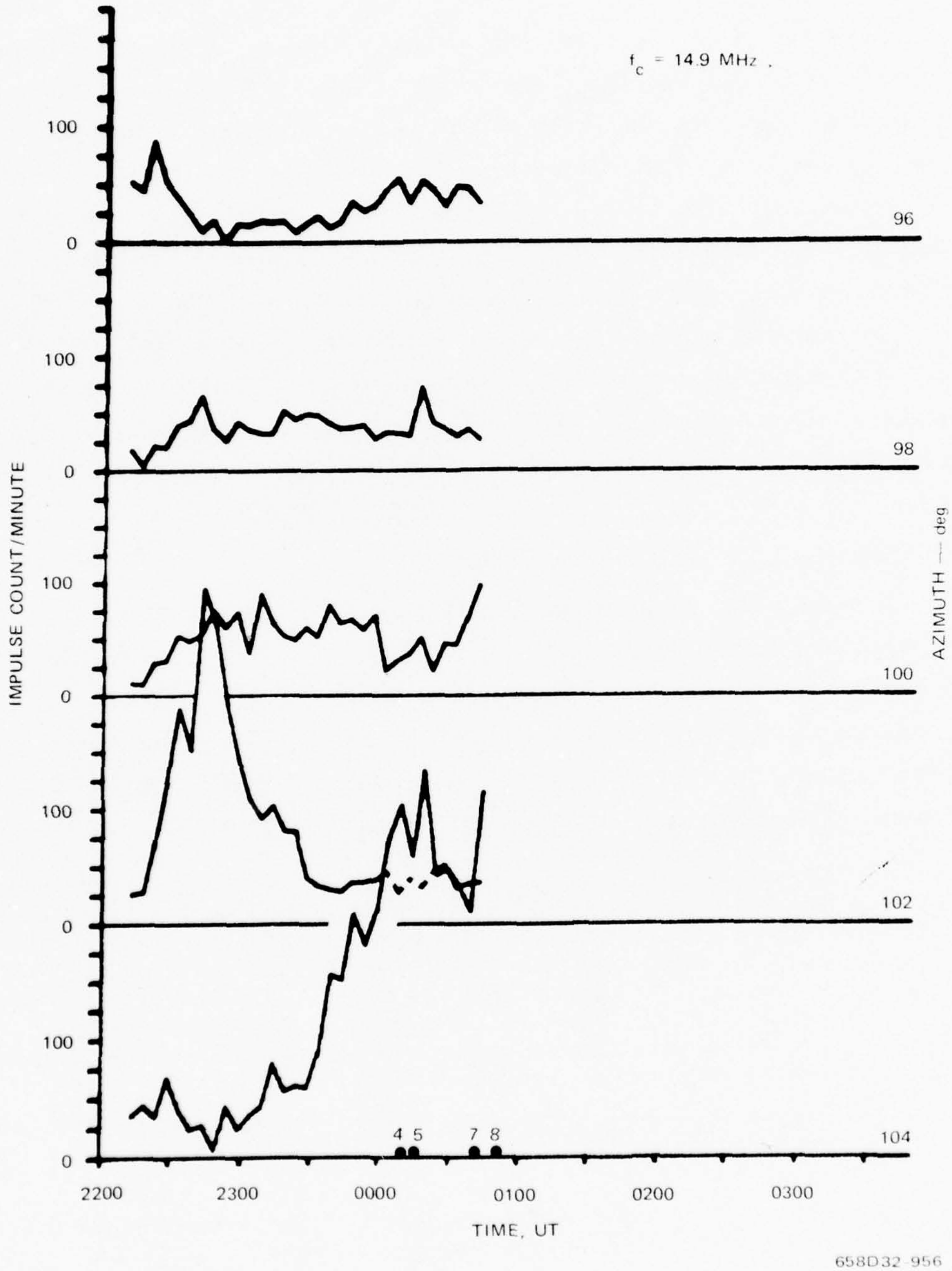

FIGURE 22 A COMPARISON OF IMPULSE COUNTS WITH SEVERE STORM SIGHTINGS — 19 MAY 1975

Analysis of the temporal and spectral details of these data shows no evidence of interference. While it is generally held that tornadoes often pass unnoticed, it would be counterproductive to excuse all data inconsistencies by Explanation 2, above. Results from other data plus the subsequent discovery of a minor antenna cabling fault strongly suggest that atmospherics from the storm that produced the tornado at Location 1 were received via a close-in antenna sidelobe.

The initial qualitative review of the data from 19 May 1975 established a significant correlation between an identifiable class of atmospherics and known remote tornadoes. In order to substantiate this, correlation data recorded on three other days were similarly analyzed.

B. Results of the Counting Process

A total of 23 hours of data collected on four days (including 19 May 1975) were analyzed. The resulting impulse counts are plotted in Figures 22 through 25. Sightings of severe weather reported either by the National Severe Storm Center or Storm Data[51] are indicated by T for tornado, F for funnel, H for hail, and G for wind gusts. Specific comments concerning these figures are given in the following:

(1) Figure 23--22 May 1975. Although not in regions scanned by the WARF antenna, many tornadoes occurred during the recording period. The lack of observations of high impulse counts suggests that the antenna sidelobe levels remained good for bearings well removed from the main lobe. The high impulse count at 2040 UT and 74°T was caused by a momentary burst of impulsive interference. In general, the counting algorithm was insensitive to low-level interference of most types.

(2) Figure 24--23 May 1975. While good temporal correlation is evident, again there are indications of close-in antenna sidelobes.

(3) Figure 25--28 May 1975. On this day, data were collected for 30 s at each of ten bearings (Format B, Table 1).

While the correlations observed in these plots are not as striking as those from 19 May, in general, high impulse counts correlate in time and approximately in azimuth with severe storm sightings.

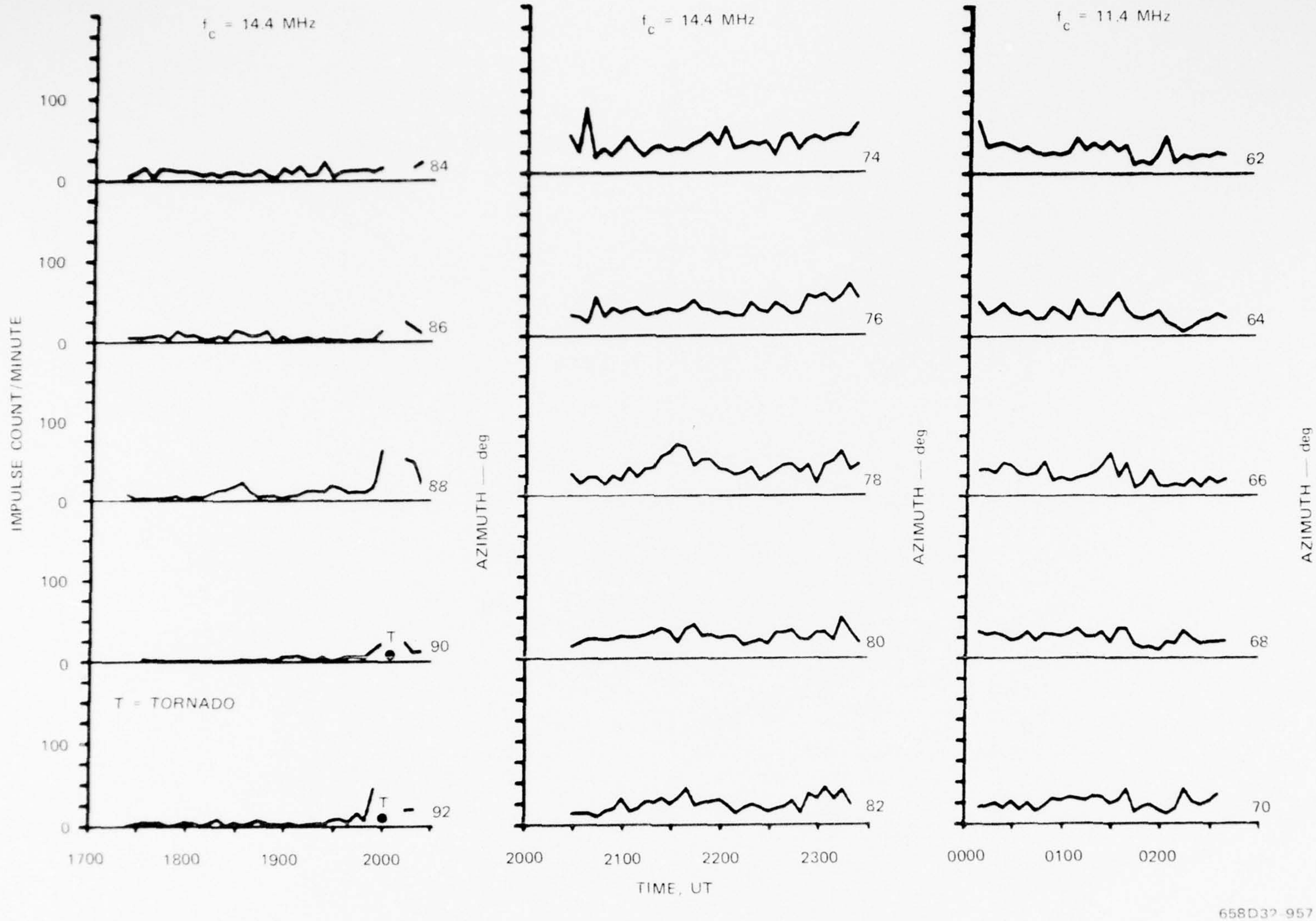

FIGURE 23 A COMPARISON OF IMPULSE COUNTS WITH SEVERE STORM SIGHTINGS — 22 MAY 1975

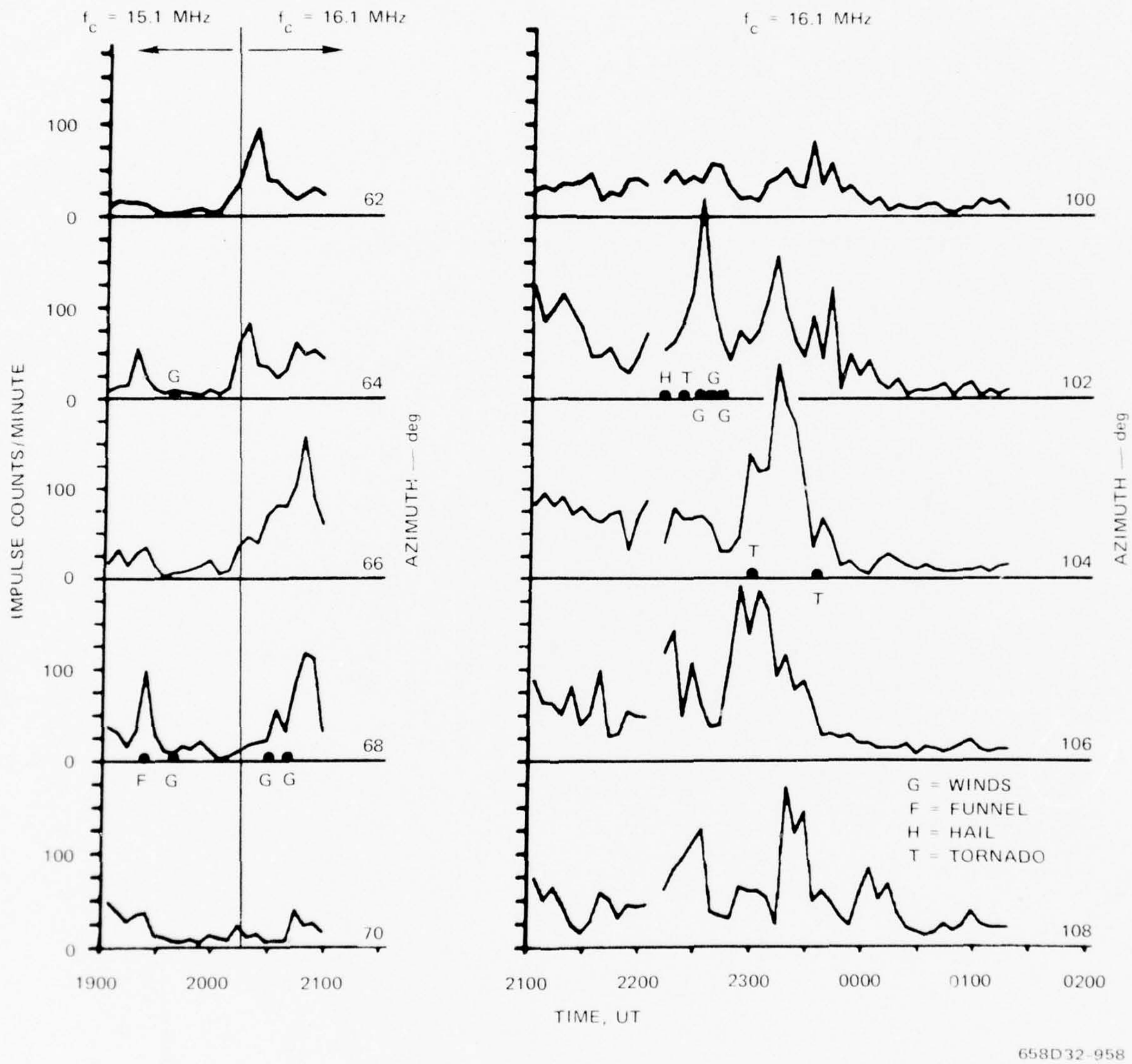

FIGURE 24 A COMPARISON OF IMPULSE COUNTS WITH SEVERE STORM SIGHTINGS — 23 MAY 1975

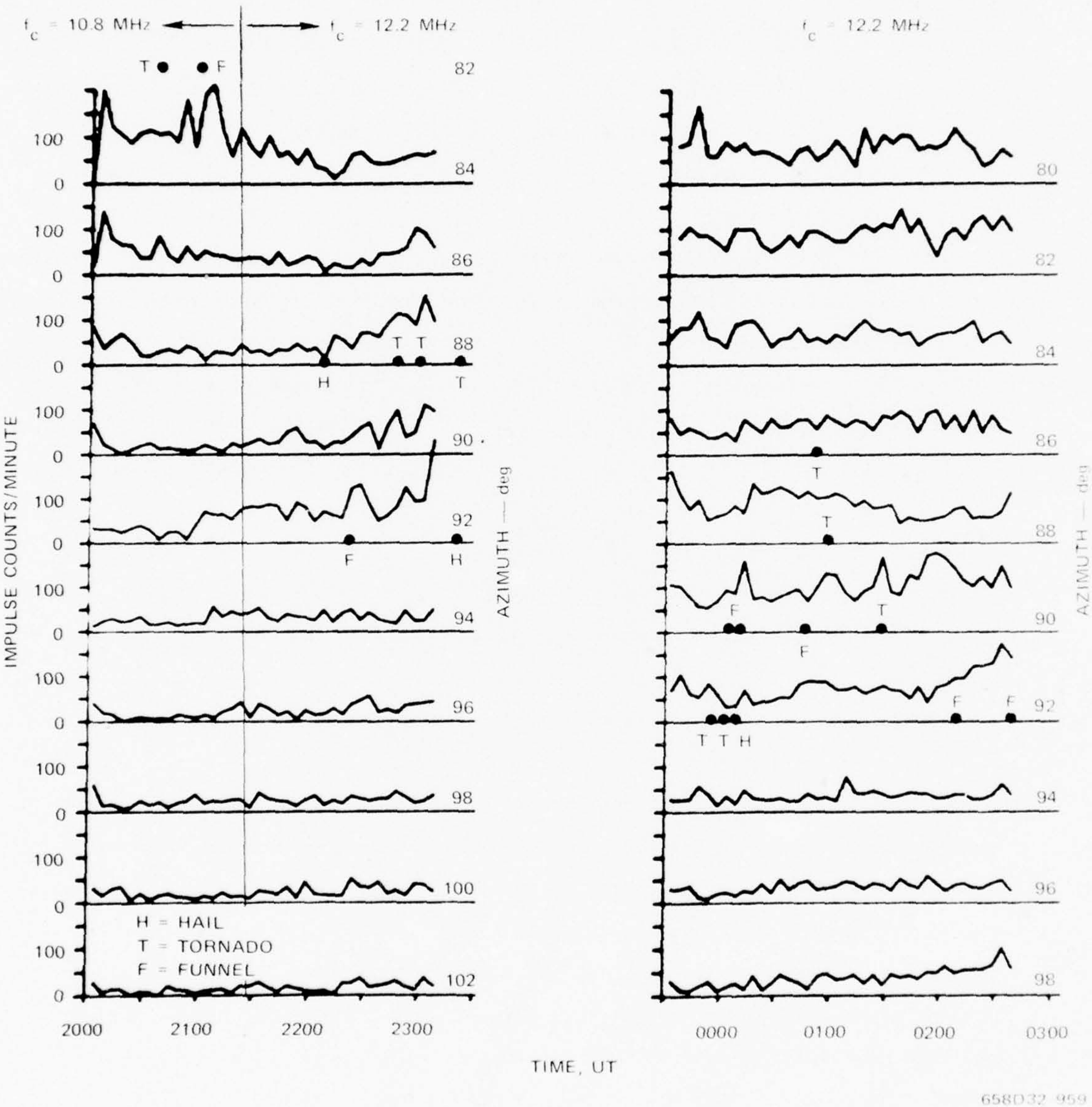

FIGURE 25 A COMPARISON OF IMPULSE COUNTS WITH SEVERE STORM SIGHTINGS — 28 MAY 1975

C. Testing the Statistical Significance of the Observed Correlations

The plots of Figures 22 through 25 show a general correlation between high impulse counts and remote severe thunderstorm events. A more reliable assessment of this correlation can be obtained through statistical analysis.

The term correlation has been loosely used to describe a relation between reception of high counts of impulses and the occurrence of midwestern severe thunderstorms. If we consider the observed impulse counts to be caused by a random process, we can precisely define correlation as a statistically meaningful difference between the probability density function governing the impulse counts observed during periods of normal storm activity and that governing the impulse counts observed during periods of severe storm activity. Specifically, impulse counts observed during severe thunderstorms have a higher mean. To prove this we must test (and reject) the hypothesis that the two random processes are identical.

1. Partitioning

To test for the equality (or difference) between the random processes generating impulse counts during periods with or without severe storm activity, the observations must first be partitioned into these two categories. Sightings are the only source of independent information available for defining these partitions. Unfortunately, severe storm events often go unnoticed. Even when observed, sightings provide incomplete information on the duration and location of each event. For these reasons partitioning errors cannot be avoided. Partitioning procedures were selected to maintain a sensitive indication of storm activity, while introducing as little bias as possible.

First, to simplify data analysis, all types of severe events (e.g., tornadoes, hail, etc.) were lumped together. Second, azimuth information was discarded to avoid partitioning difficulties caused by inexact knowledge of the spatial position of the storm and the apparent close-in sidelobes. Azimuth information was discarded by selecting the

maximum impulse count within each azimuth scan to represent that scan. Collapsing the data in this manner has the effect of making time of day the only correlation parameter.

To partition the data, a time interval corresponding to each sighting must be selected. Because the duration of events can differ, selection of a fixed partitioning interval is inexact, but the lack of detailed supporting information leaves no alternative. A partitioning interval of ±10 minutes centered about the sighting times was selected.

With the use of these partitioning rules, the data from Figures 22 through 25 were partitioned into "normal" and "severe" categories. Histograms of the resulting observations were plotted in Figure 26. These histograms show marked differences. The statistical procedure described below was used to test against the possibility that these differences could have happened merely by chance.

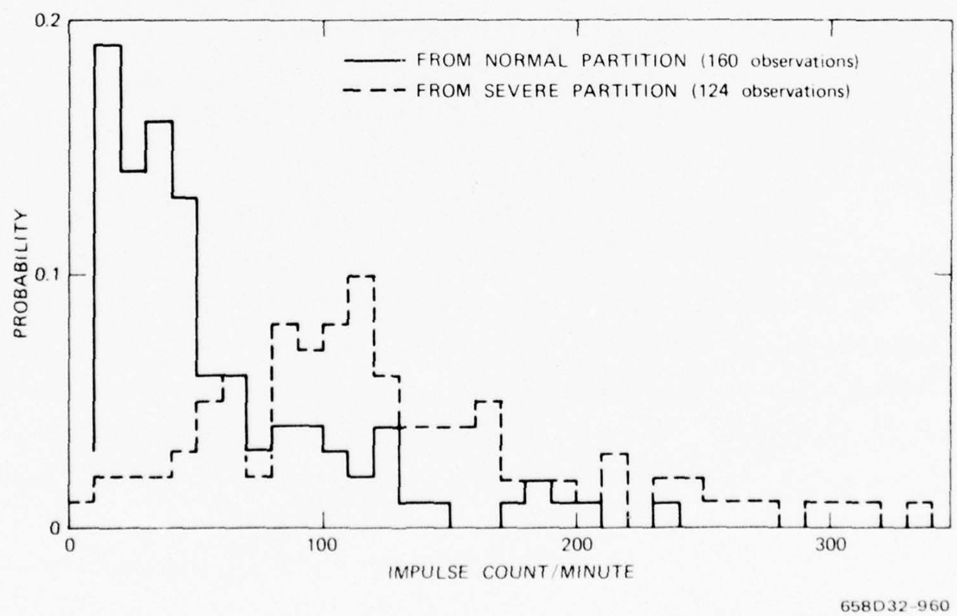

FIGURE 26 HISTOGRAMS OF IMPULSE COUNTS FOR SEVERE AND NORMAL PARTITIONS

2. Statistical Hypothesis Testing

Let the impulse counts partitioned into the normal category be labeled $X_1 \ldots X_n$. They shall be considered samples from a population, X, with probability density function $f_X(Z)$. Similarly, let the impulse counts partitioned into the severe category be labeled $Y_1 \ldots Y_m$. They shall be considered samples from a population, Y, with probability density function $f_Y(Z)$. The null hypothesis, H_o, can then be stated as follows. The probability density functions of the normal and severe populations are identical--i.e.,

$$f_X(Z) = f_Y(Z) \qquad \text{for all } Z. \tag{1}$$

The validity of the null hypothesis can be tested against the alternative, H_1, which is defined as follows. The probability density functions of the severe population is greater than that of the normal population (for at least one value of Z)--i.e.,

$$f_X(Z) < f_Y(Z) \qquad \text{for at least one } Z. \tag{2}$$

The null hypothesis is accepted or rejected by comparing a test statistic, U, (based on the observations) to a threshold, T (based on the appropriate probability distributions and the desired level of significance). The level of significance, α, determines the probability of falsely rejecting H_o. For the tests described below, an α of 0.01 was chosen. This implies that if there were truly no correlation, the chances are one in one hundred of erroneously concluding that there was a correlation.

If the probability density functions (f_X and f_Y) are known, a parametric test can be used. Since we wish to minimize the number of assumptions made, a non-parametric test of the hypothesis was chosen. While such tests are slightly less exact than their parametric counterparts, they are less dependent on assumptions and usually easier to compute.

3. A Non-Parametric Test for Correlation

The Wilcoxon Rank sum test[52] was selected as an appropriate non-parametric test of the stated hypothesis. To compute the necessary test statistic, the n observations of X and the m observations of Y are first lumped together and then ordered. A rank is assigned to each observation according to its position in the order (i.e., 1 to the smallest observation and $m + n$ to the largest). The sum of ranks, T_Y, assigned to the severe category is next computed. Under the null hypothesis the two probability density functions are equal and the ranked observations should be thoroughly mixed. Thus, under H_o it can be shown[52] that:

$$E[T_Y] = \frac{m(m + n + 1)}{2} \tag{3}$$

and

$$Var[T_Y] = \frac{mn(m + n + 1)}{12} . \tag{4}$$

For large values of m and n the distribution of the test statistic,

$$U = \frac{T_Y - E[T_Y]}{\sqrt{Var[T_Y]}} \tag{5}$$

is closely approximated by a standard normal distribution. To test H_o, the computed U is compared to a threshold value determined from the 0.01 significance level for a standard normal distribution function. Applying this test to the partitioned data resulted in rejection of H_o. Calculations used in the Wilcoxon test are summarized in Table 2. Rejecting the null hypothesis supports the conclusion that a statistically significant correlation exists between the observed impulse counts and the remote severe storm events. It should be emphasized that the

Table 2

A SUMMARY OF COMPUTATIONS FOR THE WILCOXON RANK SUM TEST

Number of counts in normal category, n	160
Number of counts in severe category, m	124
Sum of severe category ranks, T_Y	24,133
Expected mean of T_Y, $E[T_Y]$	17,670
Expected standard deviation of T_Y, $\sqrt{Var[T_Y]}$	686.44
Test statistic, U	9.42
Threshold at 0.01 significance level, T	2.33
$U = 9.42 > T = 2.33$	
Conclusion: Reject H_o	

calculated value of U is very high--more than nine standard deviations above the mean of a normal distribution. The random chance of calculating such a high value of U when H_o is true is negligible.

D. Defense of Assumptions

In this section results were presented from an experiment to determine if severe storm activity radiates an identifiable class of HF atmospherics that could be remotely detected. Statistical tests were used to show that the observations were significantly correlated with known severe storm events. It is necessary to review these results in light of the assumptions made and the possibilities of bias.

The Wilcoxon Rank sum test assumes that the two testing categories are sampled from independent populations. This assumption was clearly violated because the lack of exact control information made partitioning errors unavoidable. However, contamination caused by partitioning errors serves only to mix the two categories and hence support the null hypothesis.

Besides testing the validity of assumptions we must be careful to ensure that no systematic bias has been introduced into the tests. The method of partitioning is the major possible source of bias. The collapsing of azimuth information is one potential source. This procedure was selected because of known physical uncertainties in the data. Furthermore it can be argued that, under the null hypothesis, azimuth collapsing should not effect the outcome. A second source of possible bias comes from the selection of a partitioning interval. But as pointed out above, the use of a fixed partitioning interval is likely to mix the partitions and hence produce a conservative bias--i.e., one favoring the null hypothesis.

Based on the foregoing discussion the author considers the statistical results to be valid. It can be concluded from the data and tests presented here that the impulsive class of HF atmospherics is radiated during the occurrence of severe thunderstorm events such as tornadoes, and that this noise can be remotely detected on a directional antenna.

VII PROPERTIES OF HF ATMOSPHERICS RADIATED FROM SEVERE THUNDERSTORMS

The previous two sections established that HF atmospherics of a unique class were radiated during severe thunderstorms. In this section a comparison between these atmospherics and results from similar line-of-sight measurements is presented. Results of this comparison show that the remote observations represent a class of HF atmospherics not previously identified. The temporal characteristics of this new class of atmospherics are analyzed, and some speculation is presented as to the meteorological processes within severe thunderstorms that might generate these atmospherics.

A. Comparison of Remote and Line-of-Sight HF Atmospherics--Identification of a New Class of Atmospherics

Line-of-sight observations of HF atmospherics from severe thunderstorms have been made by Stanford,[31] Lind,[32] and Taylor.[33,34] In their experiments the total number of received atmospheric impulses were counted. Since HF atmospherics from normal lightning consist of hundreds of impulses, it is clear why counts of received impulses made by these researchers were typically very large. Stanford and Lind used this count directly to correlate with local severe storm activity. Taylor used the number of impulse bursts whose rate exceeded a selected threshold.

It was explained in Section V why, for remote measurements, the total number of received atmospheric impulses is not a sensitive measure of the severity of any single storm. Because it is not, the experiment described in Section V was designed to search for a class of severe storm atmospherics that could be extracted from the bulk of extraneous in-beam atmospherics. The class of atmospherics subsequently discovered and correlated with severe storms can be described as isolated impulses and represent only about 2% of the total atmospheric content received.

Consequently, the isolated impulse-counting algorithm was designed to reject most of the impulses that would be counted by Stanford and Lind, and to reject all of the impulse bursts measured by Taylor. Conversely, the remotely measured isolated impulses would account for only a very small fraction of the impulses measured by Stanford and Lind, and would never exceed the burst-rate criteria of Taylor. On the basis of these considerations, it can be assumed that the class of remotely received HF atmospherics described here has not been previously identified through line-of-sight measurements. It would be useful to apply these different measurement procedures to the same line-of-sight data to determine their relative sensitivity to severe thunderstorms.

B. Temporal Characteristics of the Observed Severe Storm Atmospherics

Since the severe storm HF atmospherics of the type described here have not been studied before, it is worthwhile measuring some of their characteristics. While it would be desirable to study these atmospherics in terms of their frequency spectrum, amplitude distribution, detailed waveform, etc., the available data limit analyses made thus far to the time sequence of the impulses. Still, this temporal characterization can be useful for estimating what processes might cause such unusual atmospherics. Accordingly, the time sequence of impulses was analyzed to determine if it followed a Poisson Law, as might be expected for a completely random process, or if it showed a more structured distribution as might be expected if the causal process was periodic, as some line-of-sight atmospherics measurements have indicated in the past.[27]

It follows that if the atmospherics are distributed along the time axis according to the Poisson Law, then the time intervals between atmospherics are exponentially distributed.[53] For this reason the time intervals between atmospherics were analyzed by plotting their cumulative distribution. Figure 27 plots this distribution for a one-minute sample recorded during the 19 May 1975 severe thunderstorm period. Also plotted is an idealized exponential distribution. These plots

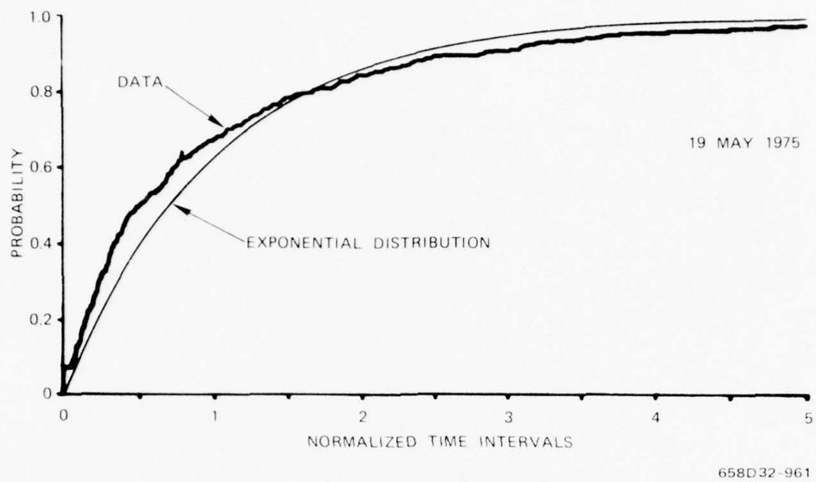

FIGURE 27 A CUMULATIVE PROBABILITY DISTRIBUTION OF THE INTERVALS BETWEEN IMPULSES SUPERIMPOSED ON AN EXPONENTIAL DISTRIBUTION

show reasonable agreement, suggesting that the atmospherics are generated by a Poisson process.

But before these atmospherics can be modeled as a simple Poisson process, it is necessary to establish that they are independent events and that their statistics do not vary with time (i.e., are stationary). This latter assumption cannot, of course, be strictly true because, as was shown in the last section, there is a definite correlation between the number of atmospherics received and the occurrence of severe thunderstorm events. However these storm events occur on a time scale of tens of minutes, and it would be useful to determine whether the statistics of these atmospherics are roughly constant for short periods (e.g., tens of seconds). For if short-term stationarity can be established, the atmospherics can be modeled as a Poisson process with a slowly varying mean.

To test for independence and short-term stationarity, two further calculations were performed on the 19 May data. First, the autocorrelation function was computed from the intervals between events (see

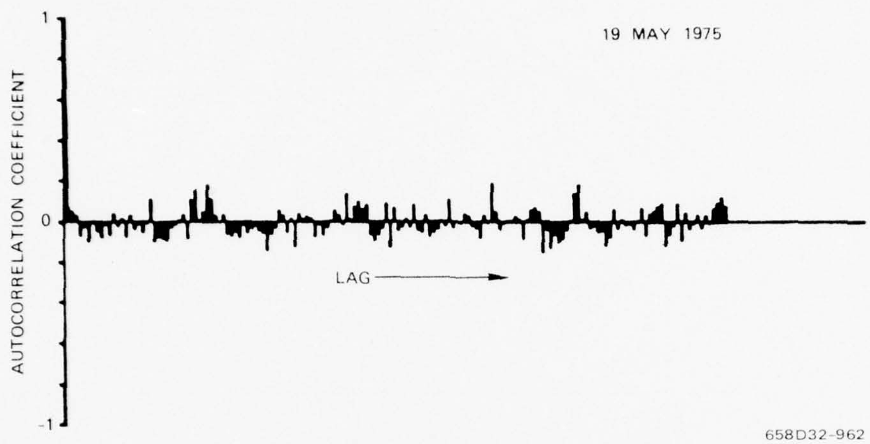

FIGURE 28 THE AUTOCORRELATION FUNCTION OF THE TIME INTERVALS BETWEEN SEVERE STORM ATMOSPHERICS

Figure 28). For an independent process this function should have small values for all lags other than zero. Second, the cumulative count of atmospherics was calculated as a function of time as shown in Figure 29. For a stationary process this plot should approximate a straight line.

The three types of temporal analyses described above were performed on 10 one-minute samples collected during the storm of 19 May 1975. All data samples gave essentially the same positive results as those depicted in Figures 27, 28, and 29. While this is not an exhaustive test, it does provide strong indications that the time sequence of remotely observed severe thunderstorm atmospherics may be generated by a Poisson process having a slowly varying mean related to the severe storm's intensity.

C. Meteorological Processes Likely to Cause the Observed Atmospherics

At this point it may be beneficial to speculate about processes within severe thunderstorms that might cause the observed atmospherics. If the source of these atmospherics can be identified, future atmospheric measurements might be used to study physical processes within

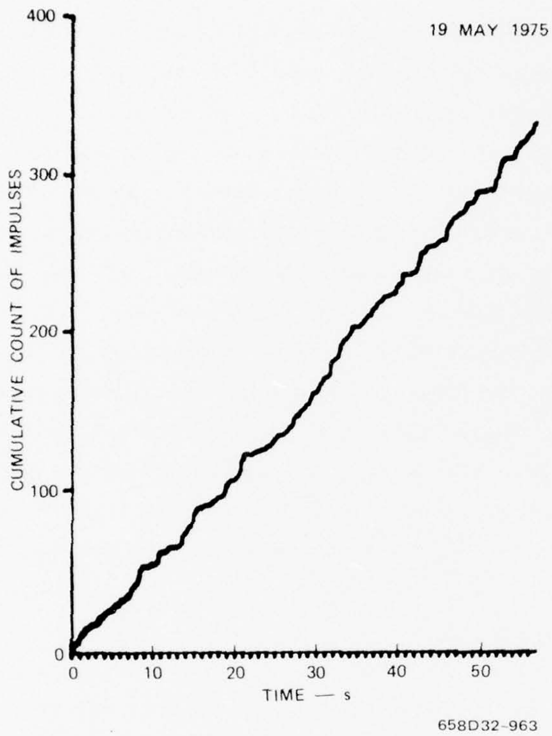

FIGURE 29 THE CUMULATIVE COUNT OF SEVERE STORM ATMOSPHERICS AS A FUNCTION OF TIME

the storm. First, let us consider what can be deduced from the measurements. The atmospherics were observed at HF and thus were likely produced from discharges of approximately 20 meters. To the 1-ms resolution achievable with the equipment used, these atmospherics appear as simple impulses, each independent of the rest. These characteristics are very different from HF atmospherics of normal lightning (comprised of many impulses following in close succession). From these observations we can assume that the lightning causing these atmospherics in severe storms is a class of frequently occurring but rather minor discharges. Two plausible generating mechanisms will be considered next.

Severe thunderstorms generally contain greater turbulence and stronger electrification than do normal thunderstorms. Because of the added turbulence, let us assume that the usual dipole distribution of electric charge within the thundercloud might be redistributed. Winds could carry smaller pockets of charge randomly about. When two oppositely charged pockets encounter one another a single relatively small discharge might occur. This process would happen throughout the cloud, creating the random atmospherics observed. Under this hypothesis the rate of atmospherics might provide information on the amount of turbulence and electrification present in the severe storm.

Under a second hypothesis the observed atmospherics would be caused by a process that generates its own free electricity. Recent Doppler radar measurements have identified concentrated regions within the storm cloud having strong wind shears and vortex motion. These localized winds can occur 10 to 20 minutes before a tornado sighting. In some instances tornadoes have been observed to originate from these vortices. It is possible that these strong winds might produce their own electricity. If they do, this could account for the short random atmospherics observed. The rate of atmospherics might then provide information on the occurrence and intensity of these localized events.

Of the two hypotheses presented above, the author considers the latter the most plausible. This is based on the following considerations. First, the turbulence theory would suggest that these atmospherics might be routinely observed in all storms. While the data presented here are inconclusive, it is the author's opinion that these atmospherics are not consistently present during normal storms. Second, the turbulence theory assumes a general process occurring throughout the storm cloud. Thus, the atmospherics would be proportional to the overall storm intensity. However, the data show strong enhancements in the number of received atmospherics occurring at the time of sighted severe storm events (e.g., see Figure 22). The observations therefore are more consistent with the wind-shear theory, which suggests that these atmospherics would be more closely linked with specific and

localized storm events. Lastly, there have been observations of lightning discharges within the actual tornado funnel.[24] Since the funnel can be considered as an extension of the in-cloud vortex, its lightning might also be caused by extreme wind shears.

Section IV discussed an HF direction-finding technique that demonstrated that the distribution of lightning within a cloud could be remotely measured. After suitable modification for processing the shorter severe storm atmospherics, this technique could be used to measure the angular distribution of these atmospherics. If they were found to be distributed over a wide region, this would support the hypothesis that they are caused by a general increase in turbulence. On the other hand, if they were found to be tightly clustered, this would support the wind-shear hypothesis.*

In concluding this section it must be emphasized that the above discussion is largely speculative. It is included to present the reader with some unproven thoughts and to demonstrate that the remote observation of these atmospherics can be useful for studying physical processes occurring within the storm cloud.

---

*It should be noted that line-of-sight direction-finding measurements have been conducted at VLF, with inconclusive results. However, it is not likely that VLF radiation is caused by the same process that generates the observed HF atmospherics.

VIII POSSIBILITIES FOR THE REMOTE STUDY OF LIGHTNING AND RELATED METEOROLOGICAL PROCESSES

The research results described in this dissertation provide new and hopefully useful information about severe-thunderstorm electricity. This research was conducted because it was recognized that the properties of a directional HF antenna were well suited for remote measurements of severe storm atmospherics. In this section we shall briefly consider how the capabilities of a directional HF antenna can be applied to gather further information that is not conveniently obtainable by other measurement techniques.

The most useful remote sensing capability of a directional antenna is the ability to select which storms within a very wide area will be monitored. For example, the WARF antenna can receive one-hop atmospherics* from storms within a region from Texas to South Dakota and the Rocky Mountains to the Mississippi River. Since most U.S. tornadoes occur within this region, the remote-sensing technique can provide a relatively inexpensive method to observe a large number of geographically separated severe thunderstorms within a single storm season. Such a measurement program could determine the percentage of severe storms exhibiting identifiable electrical activity and hence determine the value of HF atmospherics for tornado warnings.

The ability to monitor a large region is a second attractive capability of this remote-measurement technique, because wide-area measurements can help in finding and continuously monitoring severe thunderstorms. Wide-area measurements might also allow for the study of the occurrence rates of severe thunderstorms versus geographical location or meteorological conditions. Finally, in contrast with line-of-sight measurements, for the remote measurements the movements of a storm cause only a small percentage change in range and aspect angle. These

---

*This region is substantially reduced during times when blanketing sporadic-E propagation is present.

factors can allow for the observation of a thunderstorm during the entire period it is radiating identifiable atmospherics, independent of the distance the storm may travel.

For any single storm, normal summertime ionospheric propagation will limit the usable frequency band to a few megahertz.* However, this may be sufficient to gain a crude estimate of the lightning discharge length. This, in turn, could provide information about the average discharge length versus, for example, the occurrence of funnels.

Lastly, the direction-finding technique described in Section IV may be valuable for obtaining a spatial distribution of the severe storm atmospherics. No such determination of the location of discharges in the 20-meter-wavelength region has been previously attempted. It was pointed out in Section VII how such measurements might help explain the mechanisms causing these isolated atmospherics.

Thus far, I have discussed the remote-sensing properties of a directional antenna through examples having applications in severe-thunderstorm research. There may also be several uses of remote measurements of normal storms. For example, while ample line-of-sight data have been collected on over-land thunderstorms, virtually no direct measurements have been made on open-ocean thunderstorms. And those remote observations made by receiving VLF atmospherics are largely limited to the return stroke of a cloud-to-ground flash. However, remote measurements of HF atmospherics can be used to observe other lightning processes. For example, atmospherics from both cloud-to-ground and intra-cloud flashes can be received. The cloud-to-ground flashes can be identified by observation of the return stroke quenching period described in Section IV. Thus, the proportion of over-ocean flashes going to ground can be obtained. Over-land thunderstorms show a relation between the proportion of flashes going to ground and the

---

*Sporadic-E propagation or winter-day F-layer propagation could provide as much as a 2.5-to-1 usable frequency band.

storm's latitude.[54] For storms in the WARF coverage area (between 25°N and 45°N altitude) the proportion of flashes going to ground should vary from 17% to 34%. Testing this relationship for over-ocean storms might provide insight into the mechanisms causing this lightning variation with latitude.

In summary, it must be emphasized that the ability to accomplish the measurements proposed above has not been fully demonstrated. However, on the basis of the measurements that have been accomplished, the author considers these further applications as realistic possibilities. It is suggested that the remote measurement of HF atmospherics by a directional antenna can be a low-cost method of studying thunderstorm activity for a wide range of scientific and applied purposes.

IX SUMMARY AND CONCLUSIONS

A. Summary of Results

With no local thunderstorms present it was observed that strong HF atmospherics from individual lightning flashes were commonly received on a directional HF antenna. In contrast, these same atmospherics were only very weakly received on a nearly collocated omnidirectional antenna. Furthermore, the amplitude-probability distributions calculated from noise simultaneously received on these two antennas showed a significantly stronger high-amplitude (and impulsive) component for the directional antenna. These observations suggested that the directivity and sidelobe level of this directional antenna enabled the reception of atmospherics from one-hop distant in-beam lightning flashes with sufficient strength above background noise to permit measurement of their details.

Direct verification of this hypothesis was obtained during an experiment in which simultaneous measurements were recorded with the directional antenna and at a field site situated near a remote thunderstorm. The directional antenna was pointed toward the field site (and hence, the thunderstorm), which was at a one-hop distance. The simultaneous recordings showed that some of the strong atmospherics received on the directional antenna originated from the remote storm, thus marking the first time that the source of skywave HF atmospherics was precisely located. Analysis of these records demonstrated that, despite undergoing ionospheric propagation, these skywave atmospherics were received with enough strength and detail to provide usable information on individual remote lightning flashes.

By the application of digital beamforming techniques to the directional antenna, the direction of arrival of individual atmospherics was measured at 4-ms intervals with 0.06° azimuthal accuracy. This unusual measurement revealed that the direction of arrival of individual atmospherics appeared to shift, indicating changes in the horizontal positions of in-cloud radiators. For one storm, the average horizontal

dimension of the electrically active region involved in each flash was measured to be 9 ± 4 km. This is comparable to the 3-to-15-km range of values previously reported by line-of-sight observations. While there is no direct verification that the observed variations in direction of arrival were caused by changes in the radiating regions within a single flash, calibration signals received from a transmitter close to the thunderstorm showed that these unusual observations were not equipmental or ionospherically induced.

The directional antenna was next used to study atmospherics from remote severe thunderstorms. An experiment was conducted to determine if midwestern severe thunderstorms radiate identifiable atmospherics that could be remotely received. Such a class of atmospherics was observed during periods of severe storm activity. An algorithm, devised to extract this class of atmospherics from other noise, was applied to 23 hours of data collected on four days and results were compared with reports of severe storm sightings. By the use of a nonparametric statistical test, it was found that the strong presence of this class of atmospherics correlated remarkably well with the presence of severe thunderstorm events.

These observations were compared with published results of HF measurements made at line-of-sight distances from severe storms. It was found that the line-of-sight processing techniques used to estimate severe storm activity are quite different from the technique developed here. On the basis of this comparison, it is not likely that the class of remotely observed atmospherics has been previously isolated. A study of the temporal characteristics of these atmospherics revealed that they closely fit a Poisson model. Finally, it was speculated that extreme wind shears and in-cloud vortices (and perhaps even actual tornado vortices) found in severe but not normal thunderstorms are the likely generating mechanism for these unusual atmospherics.

B. Recommendations for Future Work

The current work has established the utility of a directional HF antenna for remote measurements of atmospherics and has discovered a new class of atmospherics associated with severe thunderstorms. Possible further applications of this measurement technique have already been discussed. Presented below are specific extensions of the present work applied to several different problem areas.

1. The Study of Severe Thunderstorm Atmospherics

Further remote measurements of severe storm atmospherics should be directed toward obtaining information on their amplitude distribution, frequency spectrum, location within the storm, and the relation of these characteristics with observed severe storm events. Secondly, an attempt should be made to measure this class of severe storm atmospherics at line-of-sight distances. A comparison of the sensitivity and false-alarm rates of the different algorithms used to evaluate severe storm activity would be useful.

2. The Study of Atmospherics from Hurricane Thunderstorms

Little is known about the thunderstorm activity involved with off-shore hurricanes. Since Gulf of Mexico hurricanes can come within one-hop distance of the WARF antenna, they should be monitored for any indication of the presence of unusual HF atmospherics.

3. The Effects of Atmospherics on Adaptive Beamforming

A topic currently receiving much attention is the use of adaptive beamforming to increase system performance on large HF antennas. Further characterization of the amplitude, temporal, and azimuthal properties of atmospherics received on large antennas would be of profit to this technology.

A P P E N D I C E S

Appendix A

THE USE OF WIDE-SWEEP BACKSCATTER SOUNDINGS FOR FREQUENCY SELECTION

During the past decade wide-sweep backscatter soundings have developed into a useful ionospheric diagnostic technique. Taken from one location,* these soundings provide information on current propagation conditions for frequencies in the HF band and for distances of interest. A block diagram of WARF equipment used to generate these soundings is shown in Figure A-1. An example of a wide-sweep backscatter sounding is reproduced in Figure A-2. For these soundings, backscattered energy is coded as intensity and plotted versus radio frequency and propagation time delay. Such backscatter soundings were periodically taken during the experiments described in this report. Details of the transmitted waveform and data processing necessary to produce such soundings have been described by Sweeney,[5] Barnum,[6] and Washburn.[7] Of concern here is the manner in which these soundings are used to determine an appropriate receiving frequency.

The soundings were used to choose a frequency interval, about 1 MHz wide, that would provide good propagation from a desired location or region. The relative propagation strength can be measured from the sounding if we assume the scattering cross section of the ground to be reasonably constant. This is an excellent assumption for sea backscatter and remains usable for land backscatter if localized enhancements caused by land prominences are ignored.

In the evaluation of propagation conditions for a specific location, the ionospheric reflecting height must be approximately known. This is necessary so that the ground range to the location can be converted to propagation time-delay for comparison with the backscatter sounding. An estimate of the ionospheric reflection height can be

---

*Transmitter and receiver may be slightly separated (e.g., separation for the WARF sounder is approximately 185 km).

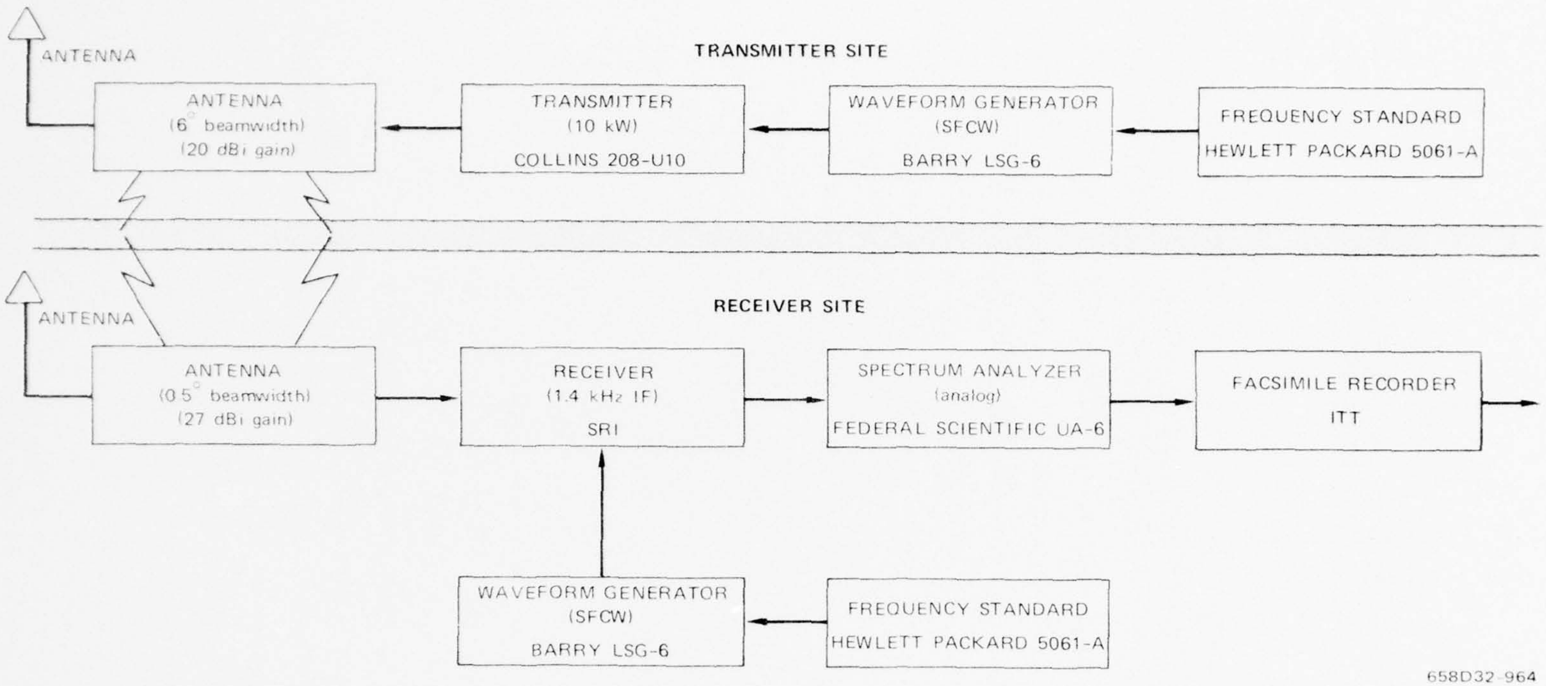

FIGURE A-1 BLOCK DIAGRAM OF WARF EQUIPMENT USED TO GENERATE WIDE-SWEEP BACKSCATTER SOUNDINGS

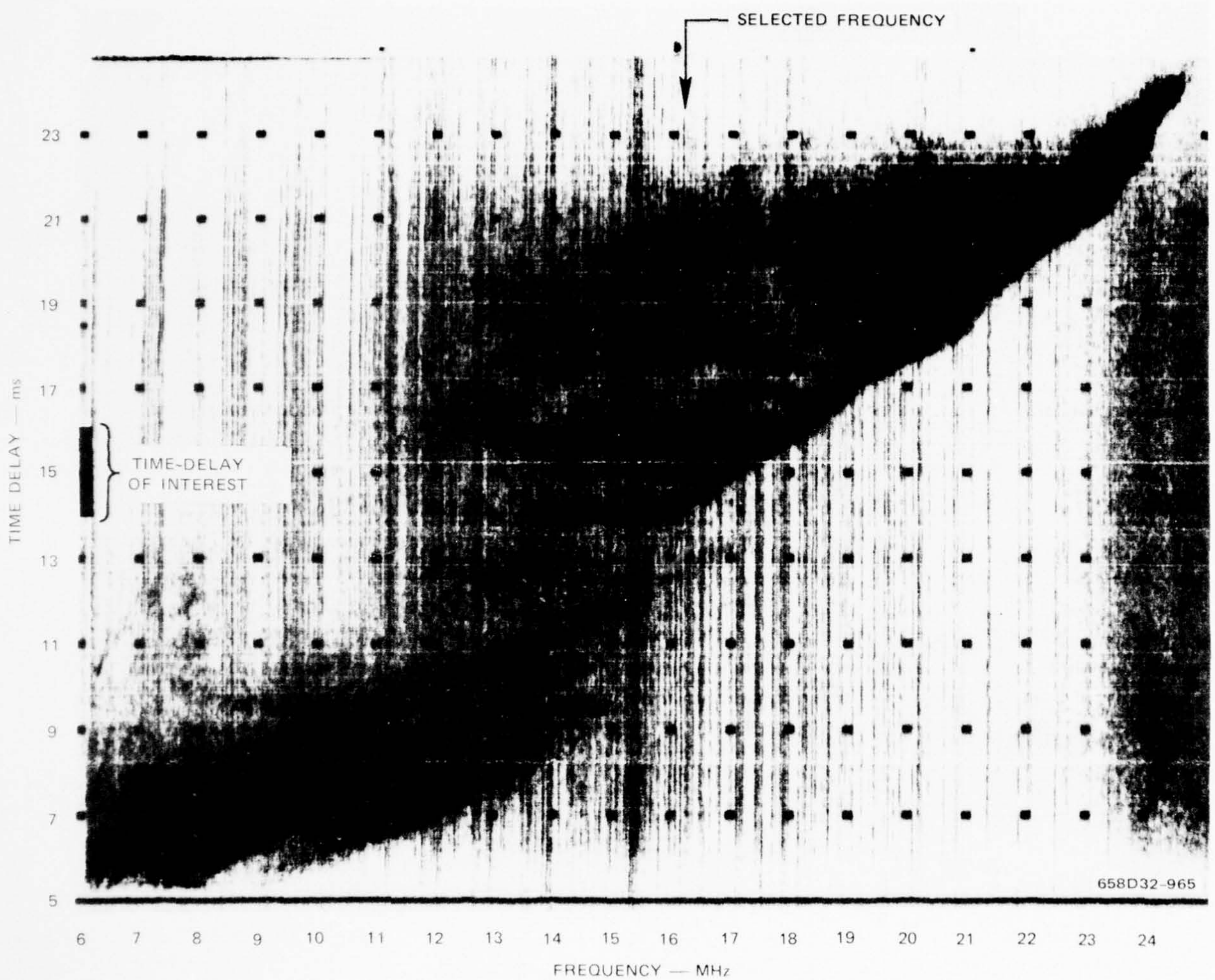

FIGURE A-2 A WIDE-SWEEP BACKSCATTER SOUNDING

obtained by identifying the propagation layer through analysis of the wide-sweep soundings or by extrapolation from heights measured directly overhead.

Once the height of reflection has been estimated, the propagation time-delay interval for a specific ground-range interval (i.e., a specified geographic region) can be determined. The sounding is used to identify the frequency interval with the strongest backscatter over the specified time-delay interval. A radio receiver is next scanned across the selected frequency interval to choose a single channel (of bandwidth 1.4 kHz) that is free of interference.

For example, the sounding of Figure A-2 was taken on 23 May when the weather watch of Figure 17 was in effect. Analysis of the sounding suggested that the principal mode of ionospheric propagation was F-layer. The overlay of Figure 17 was constructed assuming typical F-layer heights and was used to convert the geographic location of the weather watch into a time-delay interval. From the sounding of Figure A-2 a frequency band centered about 15.5 MHz was chosen as having the best propagation from the weather watch area. A clear-channel search was then conducted and a frequency of 16.09 MHz was selected for use in data collection.

Appendix B

THE ASSOCIATION OF ATMOSPHERICS RECEIVED IN CALIFORNIA WITH THOSE RECORDED UNDER A NEW MEXICO THUNDERSTORM

In Section IV, atmospherics received in California were associated with those received close to a thunderstorm in New Mexico. These two sets of data were recorded using different time standards. While an effort was made to synchronize these standards, it was recognized that a relative-time uncertainty was unavoidable. To remove this uncertainty, identifiable signatures of a strong atmospheric received in California were matched to corresponding features of the ELF waveform received in New Mexico. With this procedure, the time axis of the New Mexico data was shifted by 11 ms and this shift was then used for comparing the remainder of the five minute data sets. This shift was made in order to compensate for the 4.5-ms difference in propagation paths and for the difficulty of synchronizing to the weak and fading skywave time signal received from the National Bureau of Standards.

The introduction of this time shift introduces the possibility of bias to the association process, and it is important to establish that subsequent associations were due to a definite cause-and-effect relationship and are not a mere happenstance brought about by the arbitrary initial time shift and the chance sequence of random atmospherics.

The atmospherics received in California were presumably caused by in-beam lightning flashes. Only a fraction of these atmospherics were likely to be caused by the storm monitored in New Mexico. Clearly, the more atmospherics received in California and/or the looser the rules for association (i.e., the association time interval), the greater was the chance of a random association. Thus it was necessary to determine the likely rate of random associations based on the rate of atmospherics received in California and the time interval used for associations.

During the 5-minute data sequence the average rate of atmospherics received at WARF was less than five per second. Here each distinct atmospheric signature that could be used for making an association

AD-A044 737 STANFORD RESEARCH INST MENLO PARK CALIF F/G 20/14
OBSERVED CHARACTERISTICS OF IONOSPHERICALLY PROPAGATED HF ATMOS--ETC(U)
MAY 77 W B ZAVOLI

UNCLASSIFIED NL

2 OF 2
ADA044737

END
DATE
FILMED
10-77
DDC

(principally the abrupt return-stroke quenching) was counted separately. While the average association showed much less than a 5-ms discrepancy, for the purpose of this analysis a ±5 ms association interval was chosen. Based on these numbers, the probability, p, of randomly associating a New Mexico event with an unrelated atmospheric received in California is equal to the rate of atmospherics received, multiplied by the association interval (i.e., $5 \times 1 \times 10^{-2} = 0.05$). Assuming independent events, the number of associations, k, out of the total number of New Mexico events, N, is given in accordance with the binomial distribution:

$$P \left\{ \begin{matrix} \text{K associations} \\ \text{out of N tries} \end{matrix} \right\} = \frac{N!}{K!\ (N-K)!}\ p^K (1-p)^{N-K} \quad . \qquad \text{(B-1)}$$

During the 5-minute data set analyzed, 53 flashes occurred in the New Mexico thunderstorm, excluding the flash used to adjust the time scales. If none of the atmospherics received in California were caused by these New Mexico flashes, then Eq. (B-1) would describe the probability of K random associations with $p = 0.05$ and $N = 53$. The probability of having more than seven random associations is found to be less than 0.01. There were a total of 43 observed associations. Since there is much less than one chance in one hundred that most of the observed associations could have occurred by chance, the desired cause-and-effect relationship has been established.

Appendix C

THE WARF ANTENNA DIGITAL BEAMFORMER

Section IV of the main test describes observations of the spatial distribution of individual atmospherics. Those observations were obtained by digitally forming eight contiguous beams, each of approximately 0.5^{o} beamwidth. The equipment and processing required to accomplish this digital beamforming are described here.

Figure C-1 shows diagramatically the WARF receiving antenna and the equipment configuration used by the digital beamformer. Elements within each subarray are combined via analog means. This enables the array to be steered in the general direction of interest. The subarray beam pattern is also useful for rejecting unwanted off-axis energy. The eight-channel coherent receiver[43] and simultaneous sample and holds were built at SRI expressly for such digital beamforming applications. Table C-1 lists the pertinent parameters used for data collection and processing.

The eight channels of data were digitized and recorded for off-line analyses. During analysis the data are read back from tape and the eight beams are formed by applying a two-dimensional Fourier transform to the Data. Figure C-2 indicates the processing steps involved. Eight contiguous samples from each of the eight receiver channels are processed coherently to form a single azimuth profile. A 2048-Hz sample rate enables the calculation of independent azimuth profiles for every 4 ms of data.

Each block of data is first weighted to reduce sidelobes in the time/frequency and space/azimuth dimensions. The eight weighted samples from each channel are then Fourier transformed. This results in four complex frequency samples for each of the eight channels. Next, for the two center frequencies, a Fourier transform is applied to the data from the eight channels. Just prior to this transform the data are padded with zeros to achieve azimuthal interpolation. After the transforms the magnitudes of the data are computed and the results

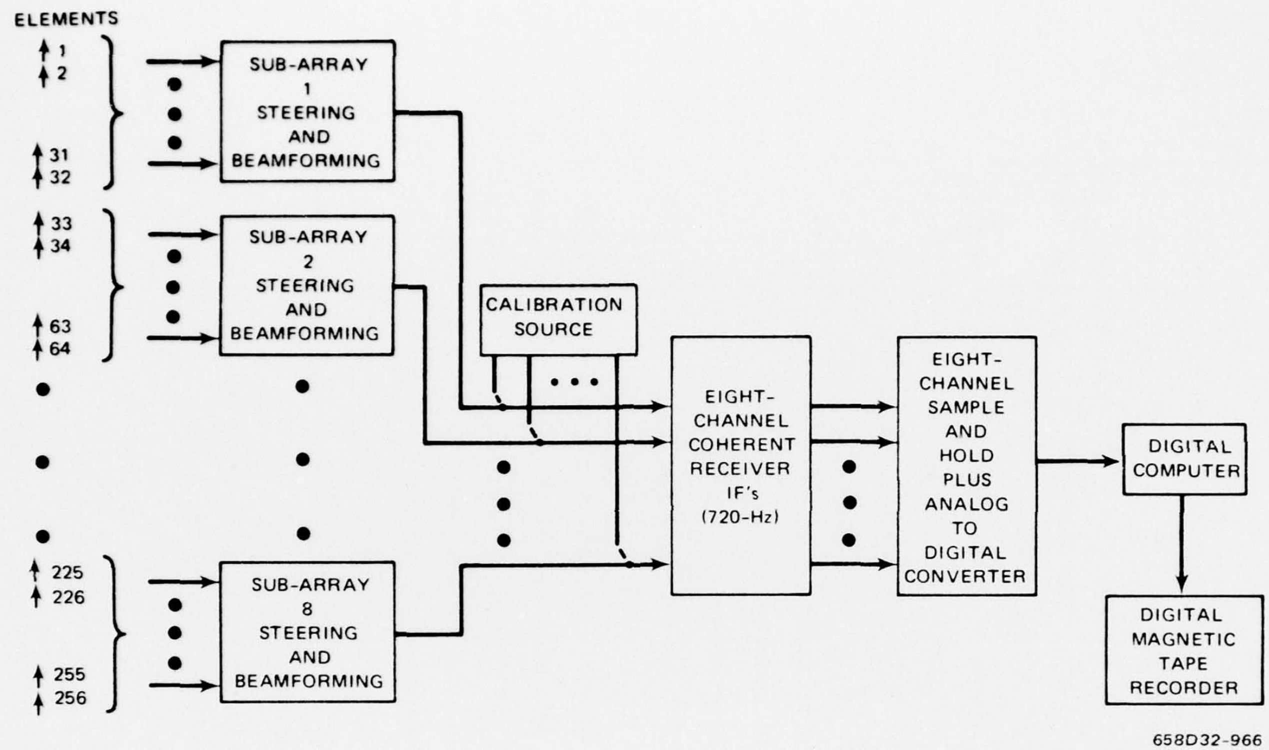

FIGURE C-1 WARF RECEIVING ANTENNA AND EQUIPMENT CONFIGURATION FOR DIGITAL BEAMFORMING

Table C-1

SUMMARY OF DIGITAL BEAMFORMING PARAMETERS

Number of subarrays	8
Receiver bandwidths	720 Hz
Sample rate per channel	2048 Hz
Temporal integration	$\sim$ 4 ms
Azimuthal resolution	$\sim 0.5^{\circ}$
Interpolation accuracy	$\sim 0.06^{\circ}$

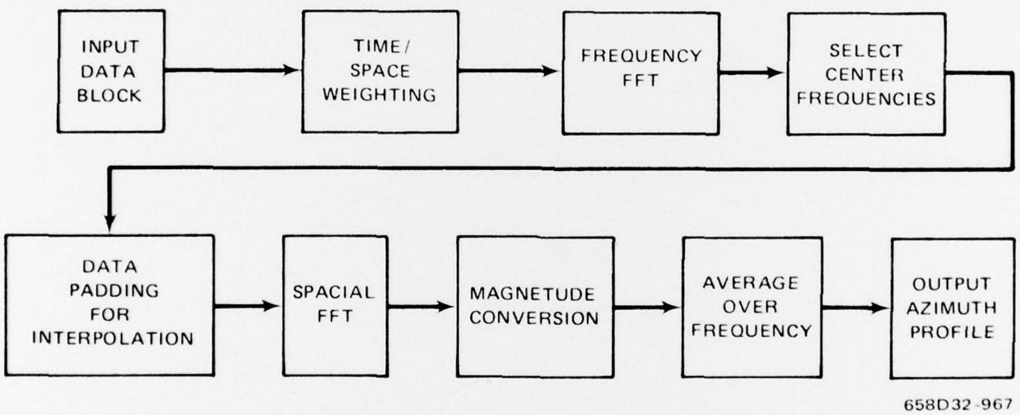

FIGURE C-2 BEAMFORMER DATA PROCESSING FOR EACH 4-ms DATA INTERVAL

from the two frequency cells are incoherently averaged. This procedure results in an interpolated estimate of the azimuthal distribution of noise received during a 4-ms period. Contiguous 4-ms data intervals are processed in an identical manner to produce the plots of amplitude versus azimuth and time shown in Figures 15, 16, and 17 of the main text.

REFERENCES

1. F. Horner, "Radio Noise from Thunderstorms," Advances In Radio Research, J. A. Saxton, ed., Vol. 2, pp. 121-204 (Academic Press, London, 1964).

2. K. Davies, Ionospheric Radio Propagation, National Bureau of Standards Monograph 80, U.S. Department of Commerce (U.S. Government Printing Office, Washington, D.C., 1965).

3. Special Facility Brochure, SRI Ionospheric Dynamics Laboratory Wide Aperture Research Facility, Stanford Research Institute, Menlo Park, California (1974).

4. SRI Remote Measurements Laboratory, Research Capabilities, Stanford Research Institute, Menlo Park, California (1976).

5. L. E. Sweeney, Jr., "Spatial Properties of Ionospheric Radio Propagation as Determined with Half-Degree Azimuthal Resolution," Technical Report 155, Contract NONR-225(64), NR 088-019, Stanford Electronics Laboratories, Stanford University, Stanford, California (1970).

6. J. R. Barnum, "The Effects of Polarization Rotation on the Amplitude of Ionospherically Propagated Sea Backscatter," Technical Report 157, Contract NONR-225(64), NR 088-019, Stanford Electronics Laboratories, Stanford University, Stanford, California (1970).

7. T. W. Washburn, "Discrete Echoes in Ionospherically Propagated Ground Backscatter," Technical Report 5, Contract N00014-70-C-0413, Stanford Research Institute, Menlo Park, California (1971).

8. D. McKinney and W. B. Zavoli, "Suppression of Impulse Noise in OTH-B Radars," Technical Report 25, Contract N00014-70-C-0413, Stanford Research Institute, Menlo Park, California (1974).

9. F. Horner, "The Reception of Atmospherics at High Frequencies," J. Atmos. Terr. Phys., Vol. 4, pp. 129-140 (1953).

10. E. Viemeister, The Lightning Book (Doubleday & Company, Inc., Garden City, New York, 1961).

11. D. J. Malan, Physics of Lightning (The English Universities Press, Ltd., London, 1963).

12. M. A. Uman, Lightning (McGraw-Hill Book Company, New York, N.Y., 1969).

13. R. A. Watson-Watt and E. V. Appleton, "On The Nature of Atmospherics I," Proc. Roy. Soc., Vol. 103, pp. 84-102 (1923).

14. E. V. Appleton and R. A. Watson-Watt, "On The Nature of Atmospherics III," Proc. Roy. Soc., Vol. 111, pp. 654-677 (1926).

15. B. F. J. Schonland, The Flight of Thunderbolts (Clarendon Press, Oxford, 2nd Ed., 1964).

16. D. J. Malan, "Radiation From Lightning Discharges and its Relation to the Discharge Process," Recent Advances in Atmospheric Electricity, pp. 557-563, L. G. Smith, ed. (Pergamon Press, New York, N.Y., 1958).

17. F. Horner, "The Relationship Between Atmospheric Radio Noise and Lightning," J. Atmos. Terr. Phys., Vol. 13, pp. 140-153 (1958).

18. F. Horner, "Narrow-band Atmospherics from Two Local Thunderstorms," J. Atmos. Terr. Phys., Vol. 21, pp. 13-25 (1961).

19. G. N. Oetzel and E. T. Pierce, "The Radio Emissions from Close Lightning," Scientific Note 10, Contract NONR-4099(00), NR 082-206, Stanford Research Institute, Menlo Park, California (1968).

20. W. Q. Crichlow, C. J. Roubique, A. D. Spaulding, and W. M. Beery, Determination of the Amplitude-Probability Distribution of Atmospheric Radio Noise From Statistical Moments, NBS Monograph 23 (U.S. Government Printing Office, Washington, D.C., 1960).

21. H. M. Hall, "A New Model for 'Impulsive' Phenomena: Application to Atmospheric-Noise Communication Channels," Technical Reports 3412-8 and 7050-7, Project SU-SEL-66-052, Stanford Electronics Laboratories, Stanford University, Stanford, California (1966).

22. K. Furutsu and T. Ishida, "On The Theory of Amplitude Distribution of Impulsive Random Noise," J. Appl. Phys., Vol. 32, No. 7, pp. 1206-1221 (July 1961).

23. L. N. Ortenburger, D. A. Schaefer, F. W. Smith, and A. J. Kramer, "Prediction of HF Noise Directivity From Thunderstorm Probabilities (U)," Proceedings of OTH Technical Review Meeting of 12-18 March 1971 (U), Vol. I: "Ionospheric Propagation (U)," Stanford Research Institute, Menlo Park, California (1971).

24. B. Vonnegut and C. B. Moore, "Giant Electrical Storms," Recent Advances in Atmospheric Electricity, L. G. Smith, ed., pp. 399-411 (Pergamon Press, New York, N.Y., 1968).

25. H. L. Jones, "A Sferic Method of Tornado Identification and Tracking," Bull. Am. Meteorol. Soc., Vol. 32, No. 10, pp. 380-385 (1951).

26. Major R. E. Beck, "Final Report Project Tornado--Sferics Phase 1957," Severe Weather Warning Center, Det 25, 6th Weather SQ(MOB), Kansas City, Missouri (1957).

27. H. L. Jones, "The Identification of Lightning Discharges by Sferic Characteristics," Recent Advances in Atmospheric Electricity, L. G. Smith, ed., pp. 543-556 (Pergamon Press, New York, N.Y., 1958).

28. D. C. Scouten, D. T. Stephenson, and W. G. Biggs, "A Sferic Rate Azimuth-Profile of the 1955 Blackwell, Oklahoma Tornado," J. Atmos. Sci., Vol. 29, pp. 929-936 (July 1972).

29. P. A. Silberg, "Passive Electrical Measurements From Three Oklahoma Tornadoes," Proc. IEEE, Vol. 53, No. 9, pp. 1197-1204 (September 1965).

30. W. G. Biggs and P. J. Waite, "Can TV Really Detect Tornadoes?," Weatherwise, pp. 120-124 (June 1970).

31. J. L. Stanford, M. A. Lind, and G. S. Takle, "Electromagnetic Noise Studies of Severe Convective Storms in Iowa: The 1970 Storm Season," J. Atmos. Sci., Vol. 28, pp. 436-448 (April 1971).

32. M. A. Lind, J. S. Hartman, E. S. Takle, and J. L. Stanford, "Radio Noise Studies of Several Severe Weather Events in Iowa in 1971," J. Atmos. Sci., Vol. 29, pp. 1220-1223 (September 1972).

33. W. L. Taylor, "Electromagnetic Radiation from Severe Storms in Oklahoma During April 29-30, 1970," J. Geophys. Res. (Ocean and Atmospheres), Vol. 78, No. 36, pp. 8761-8777 (December 1973).

34. W. L. Taylor, "Detecting Tornadic Storms by the Burst Rate Nature of Electromagnetic Signals They Produce," Ninth Conference on Severe Local Storms, American Meteorological Society, Boston, Massachusetts, pp. 311-316 (October 1975).

35. R. A. Barham and D. Mackerras, "Vertical Aerial C.I.G.R.E. Type Lightning Flash Counter," Electronics Letters, Vol. 8, No. 19, pp. 480-482 (September 1972).

36. P. Beckmann, "Amplitude-Probability Distribution of Atmospheric Radio Noise," Radio Science J. Res. NBS/USNC-URSI, Vol. 68D, No. 6, pp. 723-736 (June 1964).

37. N. Cianos and E. T. Pierce, "A Ground-Lightning Environment for Engineering Usage," Technical Report 1, Contract L.S.-2817-A3, Stanford Research Institute, Menlo Park, California (August 1972).

38. "World Distribution of Thunderstorm Days--Part I," WMO/OMM, No. 21, TP 6, World Meteorological Organization, Geneva, Switzerland (1953).

39. E. T. Pierce, "A Relationship Between Thunderstorm Days and Lightning Flash Density," Trans. Am. Geophys. Un., Vol. 49, p. 686 (1968).

40. N. D. Clarence and D. J. Malan, "Preliminary Discharge Processes in Lightning Flashes to Ground," Quart. J. Roy. Meteorol. Soc., Vol. 83, pp. 161-172 (1957).

41. E. T. Pierce, "Fields Generated by Close Lightning," Technical Note, Stanford Research Institute, Menlo Park, California (March 1974).

42. K. S. Kreielsheimer and D. Lodge-Osborn, "A Lightning Counter to Distinguish Between Ground and Cloud Flashes," Planetary Electrodynamics, S. Coroniti and J. Hughes, eds., Vol. 2, pp. 29-42 (Gordon and Breach Science Publishers, 1969).

43. A. C. Phillips and C. A. Cole, "An Eight-Channel Coherent Receiver to Support Studies of Digital Adaptive Beamforming at HF," Technical Report 24, Contract N00014-70-C-0413, NR 088-047, Stanford Research Institute, Menlo Park, California (April 1974).

44. T. Ogawa and M. Brook, "Charge Distribution in Thunderstorm Clouds," Quart. J. Roy. Meteorol. Soc., Vol. 95, pp. 513-525 (1969).

45. D. E. Proctor, "A Hyperbolic System for Obtaining VHF Radio Pictures of Lightning," J. Geophys. Res., Vol. 76, No. 6, pp. 1478-1489 (1971).

46. A. A. Few, "Thunder," Scientific American, Vol. 233, No. 1, pp. 80-90 (July 1975).

47. A. Pearson, "Operational Forecasting and Warning of Severe Local Storms," Bull. Am. Meteorol. Soc., Vol. 57, No. 4, pp. 420-423 (April 1976).

48. Severe Local Storm WARNING Service (And Tornado Statistics 1953-1973), U.S. Department of Commerce, National Oceanic and Atmospheric Administration (U.S. Government Printing Office, Washington, D.C., 1974).

49. A. Sadowski, "Forecasting Tornado Possibilities," Weatherwise, pp. 51-54 (1958).

50. R. B. Blackman and J. W. Tukey, The Measurement of Power Spectra, (Dover Publications, Inc., New York, N.Y., 1958).

51. Storm Data, U.S. Department of Commerce, National Oceanic and Atmospheric Administration, Environmental Data Service, National Climatic Center, Asheville, North Carolina (1975).

52. A. M. Mood, F. A. Graybill, and D. C. Boes, Introduction to the Theory of Statistics, 3rd Ed. (McGraw-Hill Book Company, New York, N.Y., 1974).

53. D. R. Cox and P. A. W. Lewis, The Statistical Analysis of Series of Events (John Wiley & Sons, Inc., New York, N.Y., 1966).

54. E. T. Pierce, "Latitudinal Variation of Lightning Parameters," J. Appl. Meteorol., Vol. 9, pp. 194-195 (1970).